AD-A148 684 DEVELOPMENT OF HOLOGRAPHIC PARTICLE FIELD DATA REDUCTION BY FOURIER ANALY..(U) SPECTRON DEVELOPMENT LABS INC COSTA MESA CA J D TROLINGER ET AL. 14 AUG 84 1/1

UNCLASSIFIED SDL-84-2338-03F AFWAL-TR-84-2091 F/G 14/5 NL

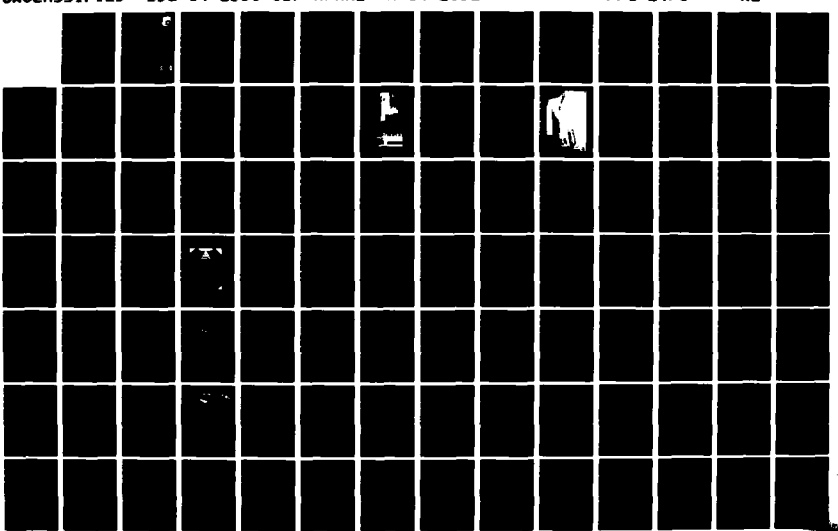

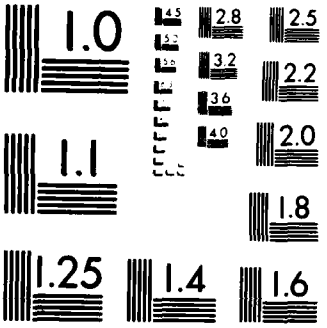

AFWAL-TR-84-2091

DEVELOPMENT OF HOLOGRAPHIC PARTICLE FIELD DATA REDUCTION BY FOURIER ANALYSIS

Dr. James D. Trolinger
Dr. Cecil F. Hess

SPECTRON DEVELOPMENT LABORATORIES, INC.
3033 HARBOR BLVD
COSTA MESA, CALIFORNIA 92626

AUGUST 1984

FINAL REPORT FOR PERIOD FEBRUARY - OCTOBER 1984

APPROVED FOR PUBLIC RELEASE; DISTRIBUTION UNLIMITED

AERO PROPULSION LABORATORY
AIR FORCE WRIGHT AERONAUTICAL LABORATORIES
AIR FORCE SYSTEM COMMAND
WRIGHT-PATTERSON AIR FORCE BASE, OHIO 45433

NOTICE

When Government drawings, specifications, or other data are used for any purpose other than in connection with a definitely related Government procurement operation, the United States Government thereby incurs no responsibility nor any obligation whatsoever; and the fact that the government may have formulated, furnished, or in any way supplied the said drawings, specifications, or other data, is not to be regarded by implication or otherwise as in any manner licensing the holder or any other person or corporation, or conveying any rights or permission to manufacture use, or sell any patented invention that may in any way be related thereto.

This report has been reviewed by the Office of Public Affairs (ASD/PA) and is releasable to the National Technical Information Service (NTIS). At NTIS, it will be available to the general public, including foreign nations.

This technical report has been reviewed and is approved for publication.

ABDOLLAH S. NEJAD, 2Lt, USAF
Aerospace Engineer
Ramjet Technology Branch
Ramjet Engine Division
Aero Propulsion Laboratory

ROGER R. CRAIG
Technical Area Manager
Ramjet Technology Branch
Ramjet Engine Division
Aero Propulsion Laboratory

FOR THE COMMANDER

FRANK D. STULL, Actg. Deputy Director
Ramjet Engine Division
Aero Propulsion Laboratory

"If your address has changed, if you wish to be removed from our mailing list, or if the addressee is no longer employed by your organization please notify AFWAL/PORT , *W-PAFB, OH 45433 to help us maintain a current mailing list".*

Copies of this report should not be returned unless return is required by security considerations, contractual obligations, or notice on a specific document.

REPORT DOCUMENTATION PAGE

1a. REPORT SECURITY CLASSIFICATION Unclassified	1b. RESTRICTIVE MARKINGS
2a. SECURITY CLASSIFICATION AUTHORITY N/A	3. DISTRIBUTION/AVAILABILITY OF REPORT Approved for public release; distribution unlimited.
2b. DECLASSIFICATION/DOWNGRADING SCHEDULE N/A	
4. PERFORMING ORGANIZATION REPORT NUMBER(S) SDL No. 84-2338-03F	5. MONITORING ORGANIZATION REPORT NUMBER(S) AFWAL-TR-84-2091
6a. NAME OF PERFORMING ORGANIZATION Spectron Development Laboratories 6b. OFFICE SYMBOL (If applicable)	7a. NAME OF MONITORING ORGANIZATION Aero Propulsion Laboratory (AFWAL/PORT) Air Force Wright Aeronautical Laboratories
6c. ADDRESS (City, State and ZIP Code) 3033 Harbor Blvd., Suite G-3 Costa Mesa CA 92626	7b. ADDRESS (City, State and ZIP Code) Wright-Patterson AFB OH 45433
8a. NAME OF FUNDING/SPONSORING ORGANIZATION 8b. OFFICE SYMBOL (If applicable)	9. PROCUREMENT INSTRUMENT IDENTIFICATION NUMBER F33615-83-C-2372
8c. ADDRESS (City, State and ZIP Code)	10. SOURCE OF FUNDING NOS. PROGRAM ELEMENT NO. 65502F; PROJECT NO. 3005; TASK NO. 20; WORK UNIT NO. 06
11. TITLE (Include Security Classification) Development of Holographic Particle Field Data Reduction by Fourier Analysis (U)	
12. PERSONAL AUTHOR(S) Dr. James D. Trolinger and Dr. Cecil F. Hess	
13a. TYPE OF REPORT Final	13b. TIME COVERED FROM 13Feb84 TO 13Oct84
14. DATE OF REPORT (Yr., Mo., Day) 14 August 1984	15. PAGE COUNT 68
16. SUPPLEMENTARY NOTATION This report is the result of a SBIR program.	

17. COSATI CODES		
FIELD	GROUP	SUB. GR.
21	08	
12	01	

18. SUBJECT TERMS (Continue on reverse if necessary and identify by block number)
Holography, Particle Sizing,
Automatic Particle Size Distribution Analysis

19. ABSTRACT (Continue on reverse if necessary and identify by block number)

The purpose of this work is to establish the feasibility of using a Fourier transform analysis to automatically extract size distribution from particle field off-axis holograms. Both experimental and theoretical studies were conducted to show that this technique is feasible. A holographic system was designed and built compatible for use with a commercially available Fourier transform analyzer and software. Holograms of a standard particle field were obtained, and the scattered light of both the particle field and its hologram were Fourier transform analyzed. The Sauter mean diameter determined by the two methods agreed to within 5%. The experimental and theoretical studies show that the prediction of the size distribution could be improved by increasing the diffraction efficiency of the hologram. This can be accomplished by producing phase holograms.

Spray holograms were also Fourier transform analyzed at various locations of the spray. Photographs of the spray are provided for comparison. The results of this phase (cont'd)

20. DISTRIBUTION/AVAILABILITY OF ABSTRACT UNCLASSIFIED/UNLIMITED ☒ SAME AS RPT. ☐ DTIC USERS ☐	21. ABSTRACT SECURITY CLASSIFICATION Unclassified
22a. NAME OF RESPONSIBLE INDIVIDUAL Abdollah S. Nejad, 2LT, USAF	22b. TELEPHONE NUMBER (Include Area Code) (513) 255-4171 22c. OFFICE SYMBOL AFWAL/PORT

BLOCK 19. ABSTRACT (Cont'd)

show that this method will yield very fast analysis of large amounts of holographic data.

The integration of holography and Fourier transform analysis will permit the acquisition and analysis of very useful data yet unattainable. Moreover, this combination will solve the long standing problem of extracting the vast quantity of data stored in holograms. This technique will find commercial applications in a variety of two-phase flows including spray combustion, rocket plume studies, explosions, and other transient events, atmospheric studies and spray diagnostics to mention a few.

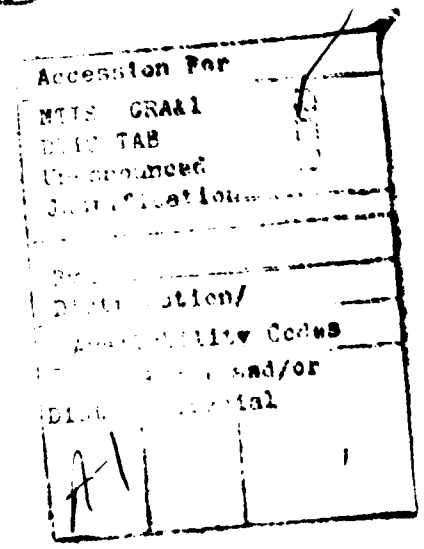

APPENDIX B

U.S. DEPARTMENT OF DEFENSE

SMALL BUSINESS INNOVATION RESEARCH PROGRAM
PHASE I—FY 1983
PROJECT SUMMARY

SDL No. 84-2338-03F

F33615-83-C-2372

FOR DOD USE ONLY

Program Office	Proposal No.	Topic No.

TO BE COMPLETED BY PROPOSER

Name and Address of Proposer

Spectron Development Laboratories, Inc.
3303 Harbor Blvd., Suite G-3
Costa Mesa, CA 92626

Name and Title of Principal Investigator

James D. Trolinger, Ph.D., Technical Director
Cecil F. Hess, Ph.D., Senior Scientist and Timothy R. Wilmot, Electro-Optical Engineer

Title of Project

DEVELOPMENT OF HOLOGRAPHIC PARTICLE FIELD DATA REDUCTION BY FOURIER ANALYSIS

Technical Abstract (Limit to two hundred words)

The purpose of this work is to establish the feasibility of using a Fourier transform analysis to automatically extract size distribution from particle field off-axis holograms. Both experimental and theoretical studies were conducted to show that this technique is feasible. A holographic system was designed and built compatible for use with a commercially available Fourier transform analyzer and software. Holograms of a standard particle field were obtained, and the scattered light of both the particle field and its hologram were Fourier transform analyzed. The Sauter mean diameter determined by the two methods agreed to within 5%. The experimental and theoretical studies show that the prediction of the size distribution could be improved by increasing the diffraction efficiency of the hologram. This can be accomplished by producing phase holograms.

Spray holograms were also Fourier transform analyzed at various locations of the spray. Photographs of the spray are provided for comparison. The results of this phase show that this method will yield very fast analysis of large amounts of holographic data.

Anticipated Benefits/Potential Commercial Applications of the Research or Development

The integration of holography and Fourier transform analysis will permit the acquisition and analysis of very useful data yet unattainable. Moreover, this combination will solve the long standing problem of extracting the vast quantity of data stored in holograms. This technique will find commercial applications in a variety of two-phase flows including spray combustion, rocket plume studies, explosions, and other transient events, atmospheric studies and spray diagnostics to mention a few.

TABLE OF CONTENTS

LIST OF FIGURES

LIST OF TABLES

INTRODUCTION

This final report documents the work conducted under Phase I of the SBIR Program, "Development of Holographic Particle Field Data Reduction by Fourier Analysis".

The objective of this program is to establish the feasibility of using a Fourier transform analysis to automatically extract size distribution from particle field off-axis holograms. Since the first application of holography for the diagnostics of particle fields, many attempts have been made to speed up the extraction of data from holograms. None of them has resulted in a successful procedure of practical utility. In the first phase of this program, we have proceeded systematically to show that the Fourier transform analysis of an off-axis particle field hologram yields very similar results to the Fourier tranform analysis of the direct particle field, thus leading to a potential solution of the problem of data extraction from particle field holograms.

In order to prove that, we chose a particle field with known invariable characteristics: a calibration reticle with a known particle distribution. These particles are chrome edged disks over a glass substrate. This particle field should yield the same result when analyzed directly or when its image, stored intermediately in a hologram, is analyzed (apart from noise and experimental errors).

A holographic system was designed and built compatible for use with a commercially available Fourier transform analyzer and software. The availability of such a system proved to be extremely cost effective

for the purpose of this research, although it might not necessarily be the optimum choice if a total system were to be developed. Several iterations of the holographic system became necessary before arriving at a fully operational system.

In addition to the calibration reticle, other more generalized particle field holograms were examined. In particular, one of these consisted of a hologram of a spray of SRC2 previously obtained with a pulsed ruby laser holocamera. This helped identify some of the limitations and requirements of integrating these two techniques and, therefore, provided very useful information for future systems.

1.0 SUMMARY OF WORK CONDUCTED UNDER PHASE I

In this section, a brief account of the effort conducted under Phase I is reported. This will provide the reader with an overall view of the program while each section will discuss in detail the various accomplished tasks.

1.1 Summary of Tasks

1. Analytical computations of resolution, S/N, type of emulsion.
2. Analytical computations of laser power requirement and exposure time for two types of holographic emulsions.
3. Design of geometry and selection of components to build a custom holographic system for this job.
4. Modify design and build three versions of a holographic system. The third version proved successful.
5. Evaluation of diffraction efficiency as a function of reference to object power ratio, illumination and exposure time, type of emulsion, and development method.
6. Evaluation of resolution using as object the 1951 USAF resolution chart.
7. Acquisition of holograms of calibration reticle.
8. Liaise with Energy and Environmental Systems Corporation to obtain use of a Malvern Systems Corporation Fourier Transform Particle Field Analyzer.

9. Characterize the Fourier diffraction analysis of the scattered field produced by the calibration reticle under various levels of laser power.

10. Interface the Malvern particle analyzer receiver and software to the holographic system. Eliminate sources of extraneous light.

11. Reconstruct and Fourier transform analyze the holograms of the calibration reticle.

12. Acquire new holograms of reticle to obtain accurate background with same collimation as the signal. Analyze the new holograms.

13. Choose adequate spray holograms from Spectron's files and perform Fourier transform analysis at various spray locations.

14. Photograph representative planes in the reconstructed image of the spray hologram for comparison with the Fourier transform analysis.

15. Final and interim reports.

2.0 HOLOGRAPHIC VERSUS DIFFRACTION FOURIER TRANSFORM DATA ANALYSIS

It is important to understand and contrast the capabilities of pulsed laser holography and real time Fourier transform analysis as applied to particle field diagnostics. In the latter case, we will be referring to commercial particle analyzers such as the Malvern Systems Corporation Particle Analyzer which provides near real time analysis of the diffraction field produced by a particle distribution. Each one is capable of providing very useful data; however, combining the two will offer the capability of obtaining and analyzing very important data which until now have been unattainable. Moreover, the combination of Fourier transform analysis with holography provides a solution to a long standing problem of how to extract the vast quantity of data which can be stored in holograms. For years, this problem had rendered the otherwise extremely powerful technique of particle field holography to be extremely limited.

In this section, the differences and similarities of both methods are summarized. As mentioned earlier, the objective of this research program is to develop an automatic data reduction process of particle field holograms. Specifically, to Fourier transform analyze the diffracted light of the reconstructed image and thus obtain the particle size distribution. Particle diagnostics can be performed directly on the diffracted light field from a particle set without using the intermediary step of holographic recording. There are, however, differences between Fourier transform analyzing the field from a dynamic event and that from a holographically reconstructed field of the event, and they will be pointed out here.

A pulsed hologram stores the image of the particle field present in a certain volume at a given instance of time. As such, it will provide useful information of both steady state and transient phenomena.

Examples of the transient processes include turbulent combustion, pulsating sprays, and explosions. The hologram becomes a permanent record of the diffraction field of particles at a certain time. Holograms obtained at different times would then provide the information needed to track the transient phenomena. These holograms can then be analyzed via the Fourier transform inversion technique to provide the size distribution as a function of time. Since the time response of the photodiodes used in the Malvern receiver is slow and their requirements for adequate light levels is high, the holograms would provide an ideal source of illumination since it is constant.

By contrast, the real time diffraction Fourier transform requires integration from many signals over a reasonable period of time (in order of seconds) to obtain adequate S/N. As such, its time resolution is limited and it provides instead a time average distribution of the particle field. For many applications, this information is quite useful and sufficient. There are other applications where the time resolution is necessary and therefore the pulse capability is required.

In turbulent combustion phenomena, laser beam steering is a problem associated with most (if not all) light scattering techniques. Since pulsed laser holography freezes the motion, the reconstructed image is stationary and can be analyzed with leisure. In explosions, the interesting phenomena may take place within a few microseconds. This time is too short to fully excite the photodiodes of the Malvern

receiver. However, holograms of the particle field can be obtained and then analyzed with the Malvern receiver. Other examples where a pulsed hologram will provide information unattainable by any other means include unsteady sprays, and shock waves.

In summary, the Fourier diffraction analysis is a slow (order of seconds) process which, until now, could only be used directly to study steady state events, or events where the time variation is not important, or events which are repetitive in nature thus allowing the accumulation of data over various cycles. This study shows that it can also be used to analyze particle field pulsed holograms thus extending its capabilities to areas of extreme interest and importance. Each technique (particle sizing holography and particle sizing by Fourier diffraction analysis) provides very useful information for a variety of phenomena. Marrying the two techniques will provide an extremely powerful tool to obtain and analyze data not attainable until now, providing all of the advantages of both procedures. Table I summarizes the characteristics and advantages of each method.

TABLE I

I. Recording the Particle Field Image in a Hologram before Analysis

Advantages

1. A large volume can be recorded in extremely short time elements with subsequent analysis of any part or all of the field.

2. Images of particles, ligaments, breakup events, can be examined in detail.

3. Fourier analysis can be applied to provide statistical data.

4. Correction for beam steering can be made.

5. The diffraction analysis can be validated by limited counting and sizing of images.

6. Highly dynamic phenomena can be analyzed.

Disadvantages

1. Data can be taken only at limited, discrete intervals.

2. An extra step is added.

II. Analyzing the Diffraction Field Directly

Advantages

1. Averages over time are provided (this is sometimes advantageous, sometimes disadvantageous.

2. It provides real time information of the particle distribution.

Disadvantages

1. Subject to beam steering in combusting flows.

2. Limited time resolution for many practical transient events.

3. Real data is not stored, therefore, it is hard to check results "a posteriori".

4. It will be fooled by ligaments and other irregularly shaped bodies.

3.0 DESCRIPTION OF APPARATUS

The apparatus used in the reported experiments consisted of three components: (1) a holographic data acquisition/reduction system; (2) the Malvern Fourier diffraction analyzer; (3) the particle field. Descriptions and design or selection criteria of these components is now given in detail.

3.1 Holographic System

Three holographic systems were designed and built on a breadboard under this program. The first was intended to obtain high resolution Fresnel holograms. We experienced noise problems partly resulting from the multiple reflections between the holographic plate and the glass substrate used as an object. The second version used a one-to-one lens relay to image the object on the holographic plate. It also used a 5 mw HeNe Laser, which proved very adequate for obtaining holograms, but was not adequate for reconstructing them. Since our goal was to build a single system for construction and reconstruction, a third version became necessary and it is described below.

This holographic system was a breadboarded, off-axis, through field system, having separate object and reference beams, as seen in Figure 1. The object beam was disturbed by a particle field, while the reference beam was unperturbed. The two beams interfere when they overlap on a holographic film plate. Figures 2 and 3 show photographs of the holographic system.

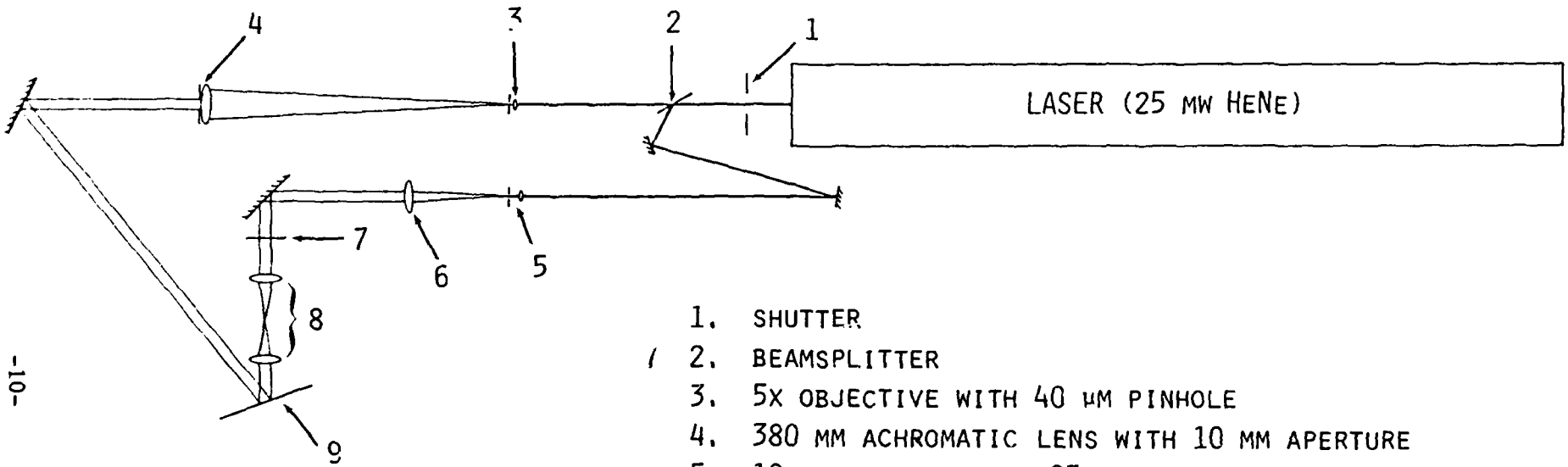

1. SHUTTER
2. BEAMSPLITTER
3. 5X OBJECTIVE WITH 40 µM PINHOLE
4. 380 MM ACHROMATIC LENS WITH 10 MM APERTURE
5. 10X OBJECTIVE WITH 25 µM PINHOLE
6. 125 MM ACHROMATIC LENS
7. PARTICLE FIELD PHOTOMASK
8. 2-50 MM OLYMPUS LENSES
9. HOLOGRAPHIC PLATE

SCALE: .13" = 1"

Figure 1. Schematic Representation of the Holographic System.

84-2338-2
84-2338-03F

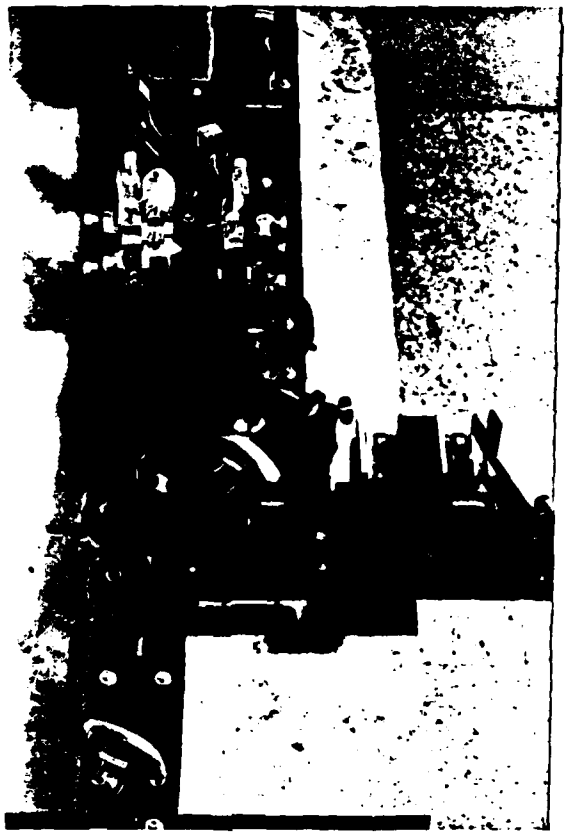

Figure 2. Photograph of Holographic System

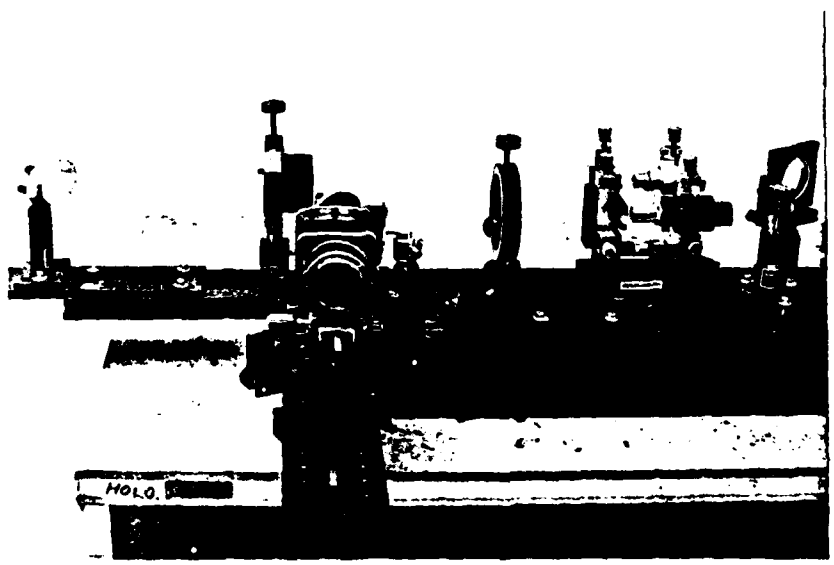

Figure 3. Photograph of Holographic System

A 25 mW Helium Neon Laser (Spectra Physics Model 107) was used as an illumination source. The beam was split with an uncoated glass beamsplitter (Newport Corporation #20B10NC.1). A split ratio of 4:1 (reference to object beam) was chosen to provide good reconstruction efficiency while remaining in the linear region of the film. The ratio was adjusted by varying the angle of incidence to the beamsplitter, thus changing the reflectivity.

The reference beam was expanded using a 5x microscope objective and spatially filtered with a 40 micron pinhole. It was collimated by a 380 mm focal length achromatic lens and apertured to a 10 mm diameter nearly uniform intensity beam. The collimated reference beam was then directed to the holographic plate, were its peak intensity was measured at 28 $\mu w/mm^2$.

A 10x microscope objective and a 25 micron pinhole were used to expand and filter the object beam. An achromatic collimating lens, with a 125 mm focal length, produced a Gaussian object beam with a diameter of 10 mm ($1/e^2$). The object beam illuminated a particle field which was imaged on the holographic plate by a 1:1 magnification lens system. This imaging system consisted of two 50 mm Olympus Lenses positioned back-to-back, connected by bellows. It collected the forward scattered radiation and the unscattered radiation and relayed them to the holographic plate. The object beam peak intensity was measured to be 6.4 $\mu w/mm^2$.

The angle between the object and reference beams (~40°) was selected to produce a fringe spacing which was larger than the grain size of the film see Appendix 2 (2500 lines/mm for 8E75), taking into

consideration some mechanical limitations. The holographic film plate was positioned such that its normal nearly bisected this angle. The object and reference beam paths were matched in distance, to within the coherence length of the laser.

3.2 The Malvern System

In its normal configuration, the Malvern Model 2600 Particle and Droplet Size Distribution Analyzer consists of a transmitter and a receiver. The transmitter provides a collimated 8 mm diameter ($1/e^2$) Gaussian beam, which illuminates a particle or droplet field. A Fourier transform lens, in the receiver, collects both the forward scattered and unscattered radiation and focuses it onto a concentric photodiode array. The scattered radiation is transformed to a series of diffraction rings at the focal plane of the lens. The 30 concentric half-ring diodes receive these data which are transferred to a mini-computer for processing. The unscattered radiation is focused on a pinhole at the focal plane of the receiving lens. This radiation illuminates a separate diode, indicating the amount of unscattered radiation.

In the experiments reported here, the Malvern's transmitter was not used. Instead, a reconstructed image of a particle field hologram was presented to the Malvern receiver. Figure 4 shows a photograph of the holographic system interfaced to the Malvern receiver which is interfaced to a microprocessor based data reduction system. The holographic recording/reconstruction system was designed to produce holograms capable of simulating the Malvern transmitter beam illuminating a particle field.

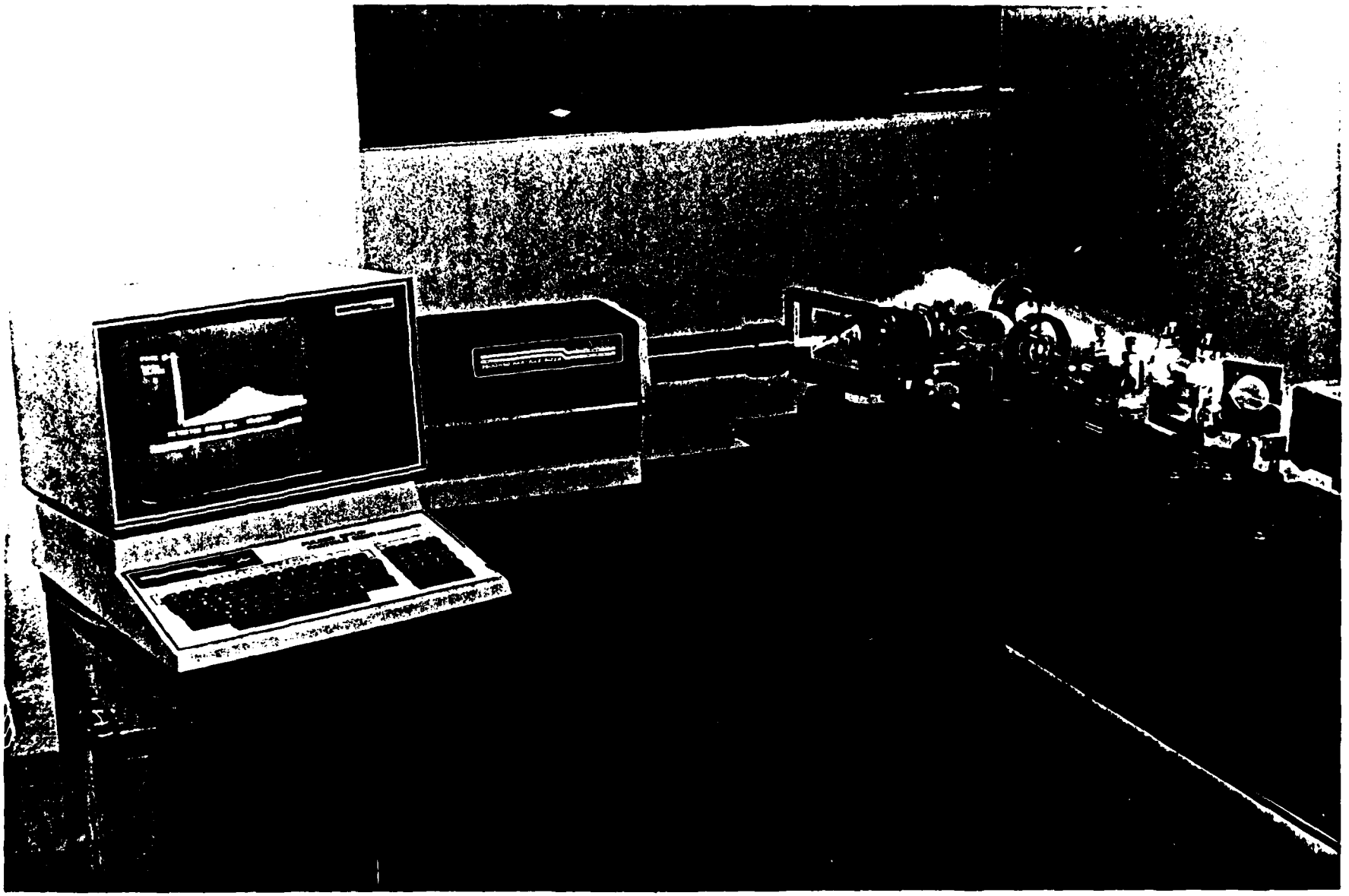

Figure 4. Photograph of Holographic System Interfaced to the Malvern Receiver.

84-2338-03F

3.3 Particle Fields

Two particle fields were used throughout these experiments. The first was a calibration photomask (Laser Electro-Optics Ltd. #RR 50-3.0-0.08-102.CF) which contains a known size distribution of circular particles. The second was a particle field hologram of a spray of synthetic fuel (SRCII) acquired in a previous program using a pulsed laser holographic system.

The photomask was chosen for two primary reasons:

1. If provided, a known and stationary particle field of which holograms could be taken with a cw laser.
2. Both the photomask and holograms of the photomask could be analyzed and compared against an absolute invariable distribution.

The calibration standard photomask consisted of a 2-dimensional sample array of 10,000 circular discs of chrome deposited on a glass substrate. The discs are randomly oriented in an 8 mm diameter sample area. The photomask contains a Rossin Rammler size distribution with $\bar{X}$ = 50 μm and a width parameter of 3.0 (Figure 5).

The particle field hologram described here containing a synthetic fuel spray was taken previously using a pulse ruby laser holocamera. The receiving optics provided a premagnification of 3:1. It has previously been determined, through existing reconstruction techniques, that the mean size of the spray droplets in this hologram lies in the range from 50 to 100 μm (depending on location) which will be interpreted as 150 to 300 μm on the magnified image of 3:1.

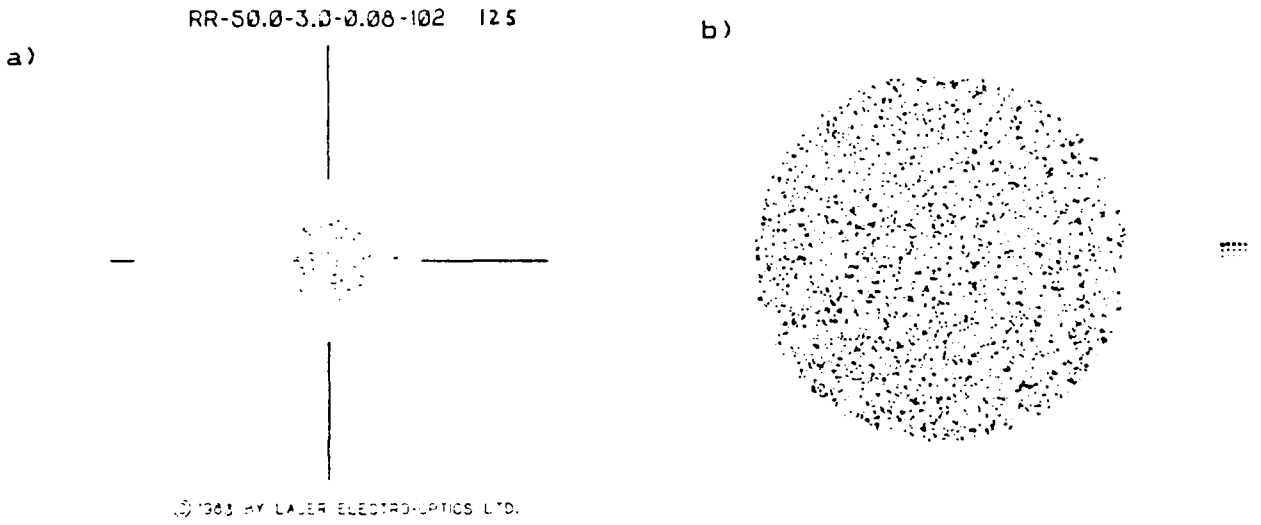

Figure 5. Photograph of calibration reticle RR-50-3.0-0.08-102-CF. (a) Magnified 1.5X. (b) Sample area and quality control array magnified 6.37X.

4.0 EXPERIMENTAL DETERMINATION OF EFFICIENCY AND RESOLUTION

The holography system was optimized, with respect to object to reference beam intensity ratio and angle of incidence, in order to produce efficient, high resolution holograms. The actual image resolution and reconstruction efficiency were determined by preliminary holograms, taken of a 1951 USAF resolution target (Newport Corporation, #RES.1). This target is similar in construction to the particle photomask consisting of chrome deposited on a glass substrate.

The preliminary holograms not only contained the object, but also optical noise. Noise contained in the particle field holograms could result in false readings by the Malvern. Scattered radiation from various optical components interfered with the object and reference beams resulting in undesirable fringes. It was necessary to eliminate or account for this noise before determining resolution and efficiency, and continuing with the experiment.

There were reflections from the film's glass substrate, which remained within the beam paths, eventually returning to the film. This condition was remedied by slightly altering the angle of the film with respect to the incoming radiation.

The glass substrate of the particle photomask caused similar reflections, requiring that its angle be slightly altered as well. A change of ~10° in both cases steered the extra reflections out of the beam path.

Another source of reflected radiation was the 2 Olympus imaging lenses. Their AR coatings are optimized for yellow light (photography)

resulting in slight reflections in the red (HeNe). Since tilting the lens would aberrate the image, we were not able to eliminate this problem. The result of these particular reflections is aberrated diffraction rings focused in the reconstructed image space. However, they could be maneuvered not to coincide with the reconstructed image, in order to reduce their effects.

An effort was made to produce efficient high resolution holograms. The efficiency was measured by reconstructing the holograms and monitoring the reconstructed beam with respect to the input power. For instance, when reconstructing hologram number 20 with a 5.5 mw (total power) reconstruction beam, the power of the resultant reconstructed beam was measured at 150 μw, showing an efficiency of ~3%. This occurred when the transmission was 20% and the beam ratio was 4:1. Most of the acquired holograms had efficiencies between 2 and 3%.

The resultant transmission of a hologram is affected during the exposure and development. The exposure time was determined from the sensitivity of the emulsion and the available laser power. Two types of emulsions were used in these studies, 8E75 and 10 E75 (AGFA-GEVAERT). The 10E75 was determined to be too sensitive for the final laser power and the available shutter speed. The 8E75 has a sensitivity of 90 ergs/cm^2, resulting in a shutter speed of 1/500 sec. To achieve the proper transmission (t_A = 16% is ideal), the holograms were developed for 6 minutes each. T_A was measured by comparing the reconstruction beam intensity in front of and behind the hologram.

The highest resolution achieved with this system was on the order of 3 μm. This was determined by visual inspection of the reconstructed

hologram of the resolution target. The fourth element of the seventh group was clearly visible with the aid of a 10x eyepiece.

At this point, it is important to mention that even though the maximum diffraction efficiency of an absorption hologram is 6.25%, phase holograms can have (in theory) efficiencies approaching 100%. There are other problems associated with phase holograms, but if these can be overcome, there is the potential to increase the power of the reconstructed image 10 to 20 times. The implication is to raise the signal to noise ratio since much of the noise is produced by light scattered from the emulsion.

4.1 Resolution When A Small Part Of The Hologram Is Used

A hologram of a volume of particles images the particles with a useful resolution which depends upon both natural limits and upon limits set by the quality of the recording. These include the following:

A. Natural (diffraction) limits

1. The diameter of the hologram.
2. The distance of the particle (or its image) from the hologram.
3. The wavelength used in the recording.

B. Quality Limits

1. The resolution of the recording medium (coherent transfer function).
2. The alignment of the hologram during reconstruction.
3. The duplications of the reference wave during reconstructon.

4. The duplication of wavelength during reconstruction.

5. Optical noise generated by the hologram, optics, and the particle field.

Quality limits can be calculated for a given recording medium and particle field. For the purposes of this discussion, it is assumed that the hologram is diffraction limited; that is, the quality of the hologram is high enough that natural diffraction limits are the limiting factors in the recording. This condition is achievable in a wide range of applications when extreme care and skill is used.

Consider a sample volume which has been illuminated by a collimated object beam of diameter D_o (See Figure 6)

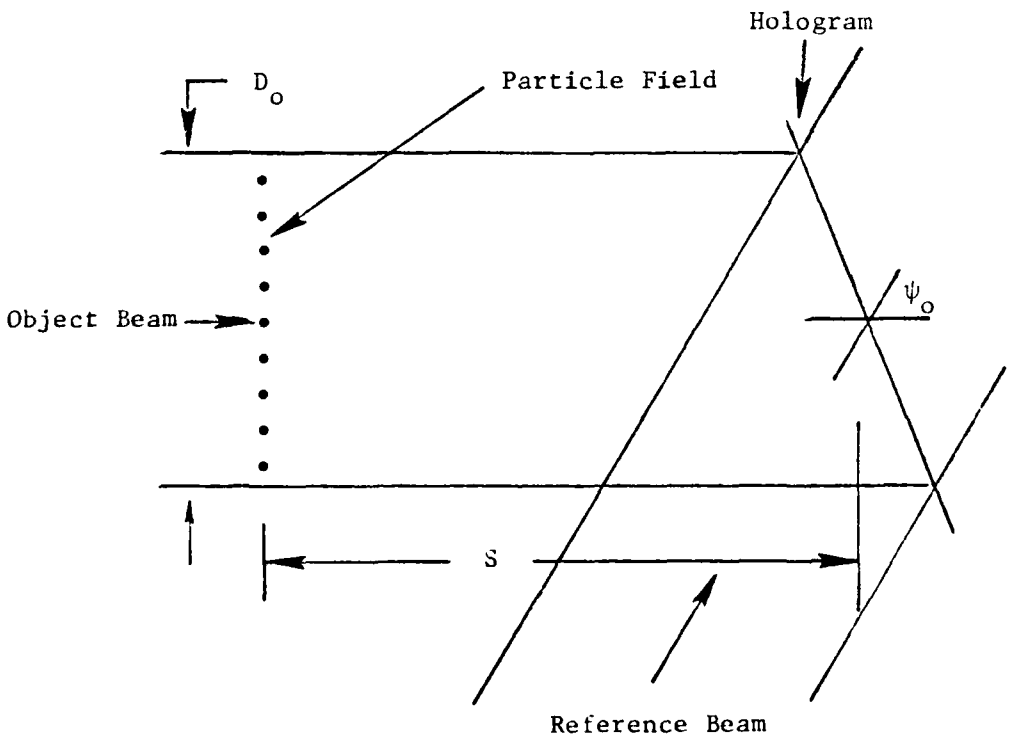

Figure 6. Recording a Hologram of a Particle Field

Typically, D_o is a diameter of about 10 cm, the diameter of a typical recording material. The diffraction limited resolution of such a hologram is

$$R = 1.25S\lambda/D_o\cos\psi_o$$

For this application, it is of interest to determine the resolution limit in an image which has been reconstructed from a small portion of the hologram. This would allow for the automated data reduction from an intentionally restricted volume within the overall sample volume (Figure 7).

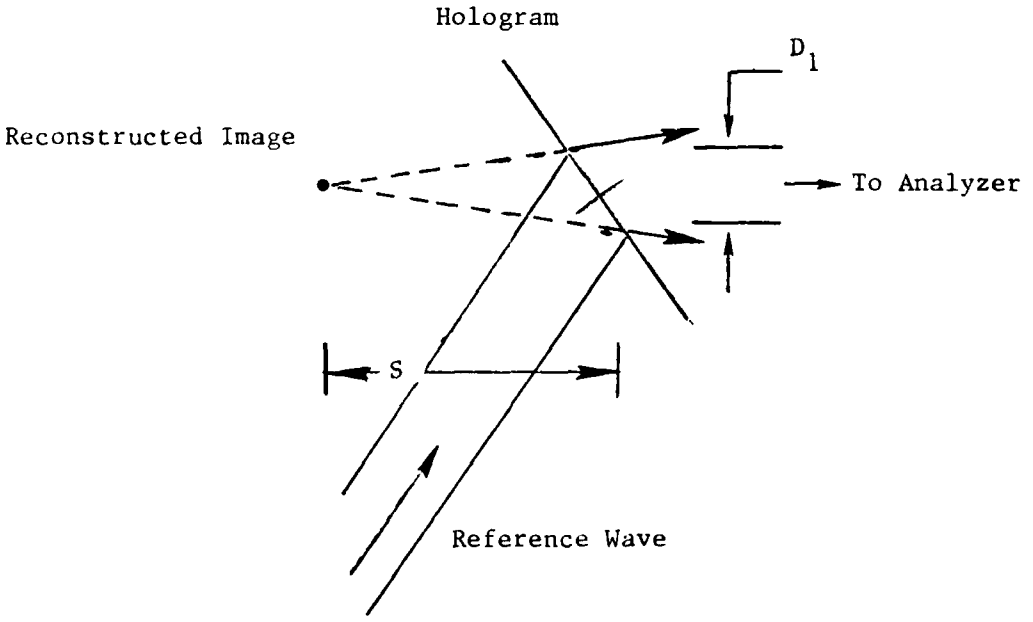

Figure 7. Reconstructing from a Restricted Portion of the Hologram

The diffraction limited resolution is now determined by the reconstruction geometry and is given by

$$R = 1.2S\lambda/D_1$$

since this by definition is the smaller of the two resolution limits caused by diffraction (the first during recording, the second during reconstruction).

Consider a typical case

$S = 5$ cm

$D = 1$ cm

$\lambda = .6$ micrometers

This gives a diffraction limited resolution of 3.6 micrometers, whereas, if the entire hologram had been used, the resolution could have been nearly five times better.

To put things in proper perspective, we have to establish the diffraction limited resolution of the Malvern receiver. Typically, this receiver uses a collection lens of 50 mm diameter and a focal length of 300 mm. In this case, R = 1.2 x 300 x 0.6/50 = 4.3 μm. Therefore, the 3.6 μm resolution obtained above is not the limiting factor.

There will be, however, cases when reconstructing a small portion of a hologram will limit the resolution and the alternative might be to reconstruct a larger portion and thus lose some spatial resolution.

5.0 RESULTS

Three particle fields were analyzed with the Malvern receiver: (1) a calibration reticle or photomask, (2) a reconstructed image of a hologram of such photomask, (3) reconstructed image of a spray hologram.

The Two different softwares provided by Malvern were used where appropriate: the Rossin Rammler and the model independent softwares. The values of $\bar{X}$ and N (defined in Section 5.3) were obtained with the Rossin Rammler distribution and are indicated in the figure legends of the model independent data.

The results are now discussed for the photomask and the spray data. A sample of these results is presented in this section while the remaining data including the outputs from the Malvern are included in Appendix 1.

5.1 Photomask Data

A total of eighteen holograms of the photomask and three holograms of the background were obtained under various conditions. As explained earlier, the objective of the parametric variation was to establish the conditions that lead to very clean, linear, and high diffraction efficiency holograms. From these, we will present the data corresponding to hologram 13 with 12 as background, and of hologram 21 with 20 as background.

There are several factors which influenced our decision to choose these holograms in addition to the ones that influence the hologram

quality. These factors are constraints imposed by the Malvern instrument to ensure adequate data reduction.

These constraints are:

1. The reconstructed image must be collimated to ensure the focus of the unscattered radiation on the center disk of the photodetector array.
2. The signal and background holograms should be acquired under the exact same conditions to ensure equal reconstructed power, equal degree of collimation, and the same traveling direction of the reconstructed image.

There are some differences between the 12/13 pair and the 20/21 pair which will now be described. Holograms 12/13 were obtained on different plate holders; the background was obtained without the photomask holder in place; the hologram was acquired with the first version of the holographic breadboard and reconstructed on the second version.

Holograms 20/21 were obtained using the same plate holder; they were also reconstructed on the same plate holder; the background was obtained illuminating the substrate of the photomask; the same version of the holography system was used for acquisition and reconstruction; a limiting mask of 5 mm was placed on the object beam to measure and correct its degree of collimation. We should, therefore, expect better results from this pair of holograms.

5.2 Procedure to Align the Malvern Receiver

The reconstructed image of the hologram must be collected by the receiving lens (we used the 300 mm in all the tests) and focused on the

diode array. Since the receiving lens of the Malvern has no focus adjustment, it is important that the reconstructed unscattered radiation be collimated and, therefore, produce a sharp focus on the hole in front of the center diode.

The receiver of the Malvern was steered until its optical axis was parallel to the reconstructed unscattered light. It was then translated vertically and horizontally until the light beam entered through the center of the lens.

The final fine adjustments were made with the adjustment screws of the receiver.

In the process of analyzing the reconstructed image with the Malvern, we established that in addition to the precautions taken during the acquisition and reconstruction of holograms 20 and 21 the plate holder should be of the type used in interferometric holography. This will ensure that the angle between the plate and the illumination beam is the same as the angle between the plate and the reference beam. If this angle changes by either tilting or rotation of the plate, the reconstructed image will follow a path slightly different than the original object. The consequence of this difference would be that the background light will focus in a different point than the unscattered light of the particle holograms.

Two different procedures of signal reconstruction were explored:

1. With the background hologram in place, the Malvern was carefully aligned until most of the light of the reconstructed image fell in the center diode. At this point, the Malvern was aligned and was not touched again.

The particle field hologram was then reconstructed and analyzed after subtracting the background.

2. In the second procedure, the Malvern receiver was aligned with the background hologram and realigned with the unscattered radiation of the particle field hologram. This procedure ensured that the unscattered radiation would fall in either case on the center diode.

This last procedure was, in general, more successful because of the slight variations encountered when repositioning the hologram on the holder. It was also necessary for analyzing the spray hologram since the reference beam used during the acquisition of this hologram was diverging, and therefore the angle of the reconstructed image would change with position on the hologram.

5.3 Energy Requirement

We established that the radiation power of the reconstructed image for the final holographic system was typically .15 mw. This can be obviously increased using a more powerful laser or increasing the diffraction efficency of the hologram. Since the Malvern apparatus uses a 2.5 mw laser, we had to establish the performance of the photodiode array at low power. The procedure consisted in illuminating the photomask with different levels of laser power. For this purpose, a variable neutral density filter was placed in front of the laser such that the total power of the light incident on the receiver varied between 50 μw and 2.5 mw. Under each one of these laser power levels we obtained a size distribution using the Rossin Rammler and the model

independent softwares. Power levels of 100 μw and more produced the same size distribution of the photomask. Power levels below 50 μw were not acceptable. It was also necessary, in order to work with the low power levels, to darken the room to reduce background radiation. Based on these results, it was expected that the 200 μw signal obtained from the reconstructed image would be more than adequate. Let us point out again that higher signal levels could be attained by reconstructing with a more powerful laser or by producing more efficient holograms. Obviously, increasing the diffraction efficiency without compromising the linearity would be the preferred choice since part of the noise comes from scatterers on the emulsion.

The photomask data are summarized on Table 2. This table shows the data obtained by analyzing with the Malvern receiver, the reconstructed holographic image of the photomask, and also the light scattered from the direct photomask. The parameters describing the size distribution are $\bar{X}$ and N which are the two parameters of the Rossin Rammler distribution which is given by:

$$V = e^{-(X/\bar{X})^N} \quad ,$$

where V is the volume fraction of drop material occurring in drops of diameter greater than X. The volume distribution is given by:

$$\frac{dv}{dx} = \frac{NX^{N-1}}{\bar{X}^N} e^{-(X/\bar{X})^N} \quad .$$

The SMD is related to $\bar{X}$ and N by the expression:

TABLE 2

PHOTOMASK DATA

Particle Field	Particle Hologram No.	Background Hologram No.	t_A	η_D	$I_{o(mw)}$	$\bar{X}$	N	Comments
Hologram of Photomask	12	13		2%	.094/.105	48.2	3.5	Aligned receiver to background only
	12	13		2%		47.4	2.6	Aligned receiver to background only
	12	13		2%		45.2	3.8	Aligned receiver to background and to particle hologram
	21	20	20%	3%	.14/.15	47.4	2.9	Data hologram slightly misplaced
	21	20	20%	3%	.14/.15	50.4	3.8	Data hologram repositioned properly
	21	20	20%	3%	.14/.15	52.1	3.9	First thing in the morning without realigning receiver
	21	20	20%	3%	.14/.15	51.5	3.7	After minor alignment
	21	20	20%	3%	.14/.15	50.5	3.8	
Direct Photomask					1.25	50.6	3.4	} 3-15-84
					0.14	50.6	3.4	
					0.12	50.8	3.2	3-12-84

$$SMD = \frac{\bar{X}}{\Gamma(1 - \frac{1}{N})}$$

To illustrate the effect of $\bar{X}$ and N on the size distribution, Figure 8 shows two volume distributions corresponding to $\bar{X}$ = 50 and N = 3 and 3.5. Large values of N correspond to narrow distributions.

5.4 Model Independent Data

The photomask and its holographic reconstructed image were also analyzed using the model independent software of Malvern. The histograms of the size distribution produced by this software will be related to the energy distribution over the photodiode ring array. As mentioned earlier, one of the difficulties encountered in processing the holographic data stemmed from the inaccuracy in repositioning the hologram. Some of the unscattered radiation would miss the central diode and illuminate the second diode. This will show as a bin in the large size band. Figures 9 and 10 correspond to reconstructed holograms (20/21) and illustrate this problem. The last column shows the light measured in each of fifteen pairs of diode rings. For instance, on Figure 9 the maximum light level (2047) is measured in the 30.3 to 39.0 μm band and this level drops toward the larger size bands only to increase again to 402 in the band of 261.6 to 564.0 μm. A similar behavior can be observed on Figure 10.

Figures 11 and 12 correspond to direct measurements of the photomask. Here the peak measured light energy also falls in the 30.3 to 39 μm size band. However, the histograms are very smooth and don't

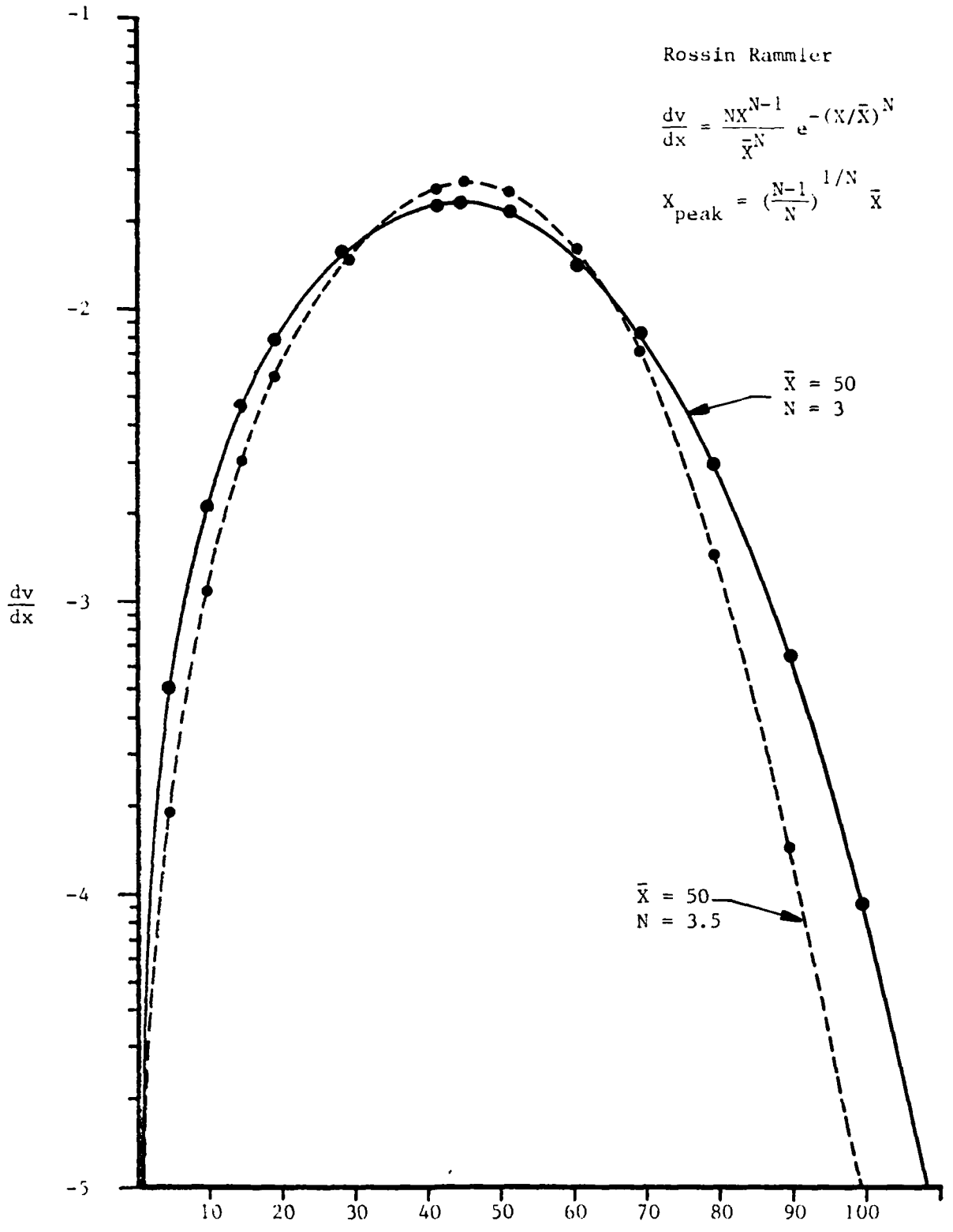

Figure 8. Effect of N On Rossin Rammler Volume Distribution.

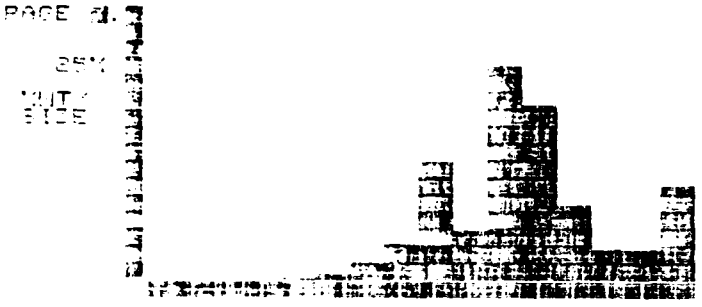

MALVERN 2600/3600 PARTICLE SIZER VF.3

MALVERN INSTRUMENTS LTD,SPRING LANE,MALVERN,ENGLAND.

PRINTING RESULTS FROM DATA BLOCK 2

TIME 09-32-09 RUN NO. 13 LOG ERROR = 6.26

SAMPLE CONCENTRATION = 0.0506 % BY VOLUME
OBSCURATION = 0.12

SIZE BAND UPPER	SIZE BAND LOWER	CUMULATIVE WT BELOW	WEIGHT IN BAND	CUMULATIVE WT ABOVE	LIGHT ENERGY COMPUTED	LIGHT ENERGY MEASURED
564.2	331.0	88.8	11.2	0.0	963	402
331.0	194.1	85.5	3.4	11.2	438	834
194.1	113.8	82.1	3.6	14.5	615	675
113.8	66.7	78.6	3.9	17.9	686	547
66.7	39.1	73.4	5.2	21.4	1260	1071
39.1	22.9	69.4	4.0	26.6	1260	1071
22.9	13.4	50.6	18.8	30.6	1673	1556
13.4	7.9	27.3	23.2	49.4	1673	1556
7.9	4.6	21.5	5.8	72.7	1994	1010
4.6	2.7	7.9	13.6	78.5	2042	2047
2.7	1.6	3.5	4.4	92.1	2034	1517
1.6	0.9	1.4	2.1	96.5	2047	1367
0.9	0.5	0.8	0.6	98.6	1397	1089
0.5	0.3	0.3	0.5	99.4	857	881
0.3	0.2	0.1	0.1	99.7	1029	699
0.2	0.1	0.1	0.1	99.9	1003	587
0.1	0.0	0.0	0.0	99.9	755	530

Figure 9. Size histogram of reconstructed Hologram 21 using Hologram 20 as background. Model independent software. The total energy level is I_o = 0.14 mw for the particle hologram and I_o = 0.15 mw for the background hologram. The corresponding Rossin Rammler parameters are X = 51.5, N = 3.7.

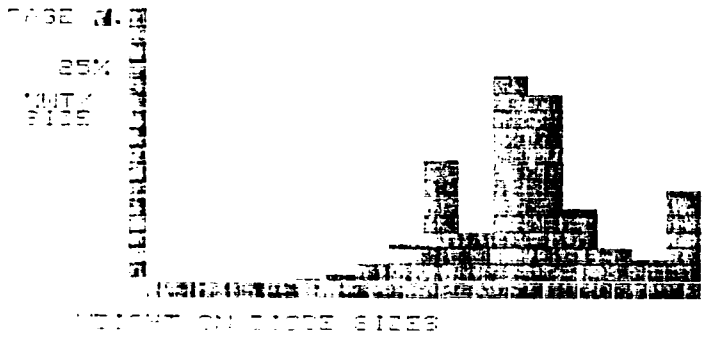

MALVERN 2600/3600 PARTICLE SIZER VF.3

MALVERN INSTRUMENTS LTD,SPRING LANE,MALVERN,ENGLAND.

PRINTING RESULTS FROM DATA BLOCK 4

TIME 08:50:30 RUN NO. 38 LOG ERROR = 0.28

SAMPLE CONCENTRATION = 0.0296 % BY VOLUME
OBSCURATION = 0.20

SIZE BAND UPPER	SIZE BAND LOWER	CUMULATIVE WT BELOW	WEIGHT IN BAND	CUMULATIVE WT ABOVE	LIGHT ENERGY COMPUTED	LIGHT ENERGY MEASURED
554.0	381.6	89.0	11.0	0.0	337	389
381.6	150.4	98.4	2.6	11.0	415	203
150.4	118.3	92.0	3.5	15.6	586	279
118.3	84.3	74.0	8.3	17.3	358	568
84.3	64.6	52.3	21.7	26.0	1225	1076
64.6	50.2	28.6	24.1	47.7	1612	1465
50.2	38.9	22.8	5.8	71.8	1925	963
38.9	30.3	8.0	14.3	77.4	1998	2047
30.3	23.5	3.7	4.3	91.7	2025	1525
23.5	18.5	1.5	2.2	96.0	2047	1380
18.5	14.5	0.6	0.9	98.5	1392	1102
14.5	11.4	0.2	0.4	99.4	850	687
11.4	9.0	0.1	0.1	99.7	1021	696
9.0	7.1	0.0	0.1	99.8	900	580
7.1	5.6	0.0	0.0	100.0	693	481

Figure 10. Size histogram of reconstructed Hologram 21 using Hologram 20 as background. Model independent software. The total energy level is I_o = 0.14 mw for the particle hologram and I_o = 0.15 mw for the background hologram. The corresponding Rossin Rammler parameters are $\bar{X}$ = 50.5, N = 3.8.

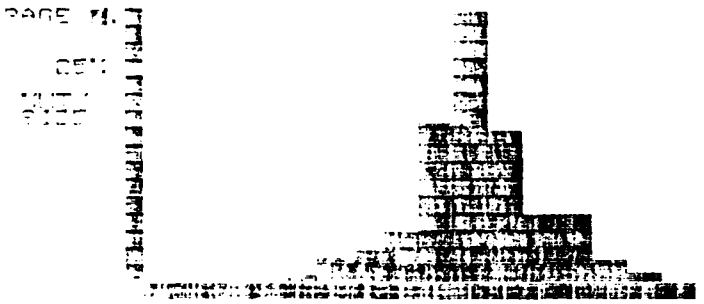

MALVERN 2600/3600 PARTICLE SIZER VF.3

MALVERN INSTRUMENTS LTD,SPRING LANE,MALVERN,ENGLAND.

PRINTING RESULTS FROM DATA BLOCK 10

TIME 13-33-20 RUN NO. 37 LOG ERROR = 4.43

SAMPLE CONCENTRATION = 0.0133 % BY VOLUME
OBSCURATION = 0.13

SIZE BAND UPPER	VOLUME	CUMULATIVE WT BELOW	WEIGHT IN BAND	CUMULATIVE WT ABOVE	LIGHT ENERGY COMPUTED	LIGHT ENERGY MEASURED
[illegible]	861.8	100.0	0.0	0.0	161	115
[illegible]	150.4	[illegible]	1.2	0.0	[illegible]	234
100.3	116.3	96.2	2.5	1.3	440	415
112.3	84.3	[illegible]	[illegible]	3.8	651	675
[illegible]	[illegible]	[illegible]	[illegible]	11.6	951	926
[illegible]	[illegible]	[illegible]	17.5	19.2	1323	1391
[illegible]	[illegible]	31.4	31.4	36.7	1748	1773
[illegible]	[illegible]	10.7	10.7	68.2	2047	2047
[illegible]	[illegible]	[illegible]	5.9	86.8	2019	1952
13.5	13.5	4.0	3.3	92.7	1694	1576
14.5	14.5	1.0	2.8	96.0	1154	1224
11.4	11.4	0.3	0.3	98.8	1032	973
[illegible]	3.1	0.1	0.0	99.0	875	758
[illegible]	5.2	0.0	0.0	99.0	610	601
[illegible]	5.0	0.0	0.0	100.0	472	487

Figure 11. Size histogram of directly measured photomask using the glass substrate as background. Model independent software. I_o = 1.25 mw. The corresponding Rossin Rammler parameters are X = 50.6, N = 3.4

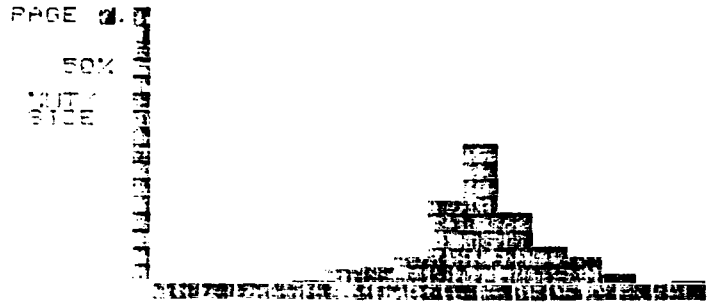

MALVERN 2600/3600 PARTICLE SIZER VF.3

MALVERN INSTRUMENTS LTD,SPRING LANE,MALVERN,ENGLAND.

PRINTING RESULTS FROM DATA BLOCK 11

TIME 13-41-40 RUN NO. 33 LOG ERROR = 4.37

SAMPLE CONCENTRATION = 0.0130 % BY VOLUME
OBSCURATION = 0.13

SIZE BAND UPPER	SIZE BAND LOWER	CUMULATIVE WT BELOW	WEIGHT IN BAND	CUMULATIVE WT ABOVE	LIGHT ENERGY COMPUTED	LIGHT ENERGY MEASURED
564.0	281.8	93.4	0.6	0.0	155	175
281.8	150.4	93.0	0.4	0.6	283	248
150.4	112.8	92.7	2.3	1.0	423	417
112.8	84.3	90.5	6.2	3.3	600	640
84.3	64.6	84.3	8.6	9.5	830	836
64.6	50.2	75.8	16.3	18.1	1310	1274
50.2	38.0	59.5	16.3	34.4	1745	1781
38.0	28.1	43.2	16.6	50.7	2047	2047
28.1	21.1	26.6	9.1	66.3	2018	1956
21.1	15.8	17.5	3.1	75.4	1822	1588
15.8	11.4	14.5	3.0	78.5	1558	1238
11.4	8.1	11.4	2.1	81.5	1243	866
8.1	5.8	9.1	2.3	83.6	870	743
5.8	4.1	6.8	2.3	85.9	492	598
4.1	2.9	4.5	2.3	88.2	501	501

Figure 12. Size histogram of directly measured photomask using the glass substrate as background. Model independent software. I_o = 0.14 mw. The corresponding Rossin Rammler parameters are X = 50.6, N = 3.4

84-2338-03FF/4

exhibit the added bin at the large size band (which correspond to the inner diodes).

The use of a precision holographic plate holder will reduce this problem considerably. Appendix 1 contains the remaining data.

5.5 Spray Hologram Data

A hologram of a spray field of synthetic fuel (SRCII) previously acquired with a pulse ruby laser was then analyzed. This hologram was obtained using (almost) uniform object and reference beams and a pre-magnification of 3. To best simulate the conditions normally used by the Malvern, a Gaussian beam of 6 mm diameter ($1/e^2$) was used for reconstruction. The reconstructed image had a total power of about 0.25 mw and a (almost) Gaussian intensity profile. The divergence of the illuminating reconstruction wave was controlled to produce a well collimated reconstructed wave.

Three regions of the hologram were reconstructed and analyzed with the Malvern receiver, and a region without spray was used to obtain the background information. These data are shown on Figure 13. It is important to realize that since the hologram was acquired with a 3:1 magnification, the actual droplet size is 1/3 of that shown.

Figure 13 shows a photograph of a given plane of the 3-D hologram, and inserts corresponding to the locations where data were acquired. Notice that the mean value changed from 285 μm (actual size 95 μm) at the edge of the spray to 165 μm (actual size 55 μm) at the center. This is the typical trend of sprays formed by simple pressure nozzles in which more large droplets are found at the edge of the spray.

FOURIER DIFFRACTION ANALYSIS OF A FUEL SPRAY HOLOGRAM

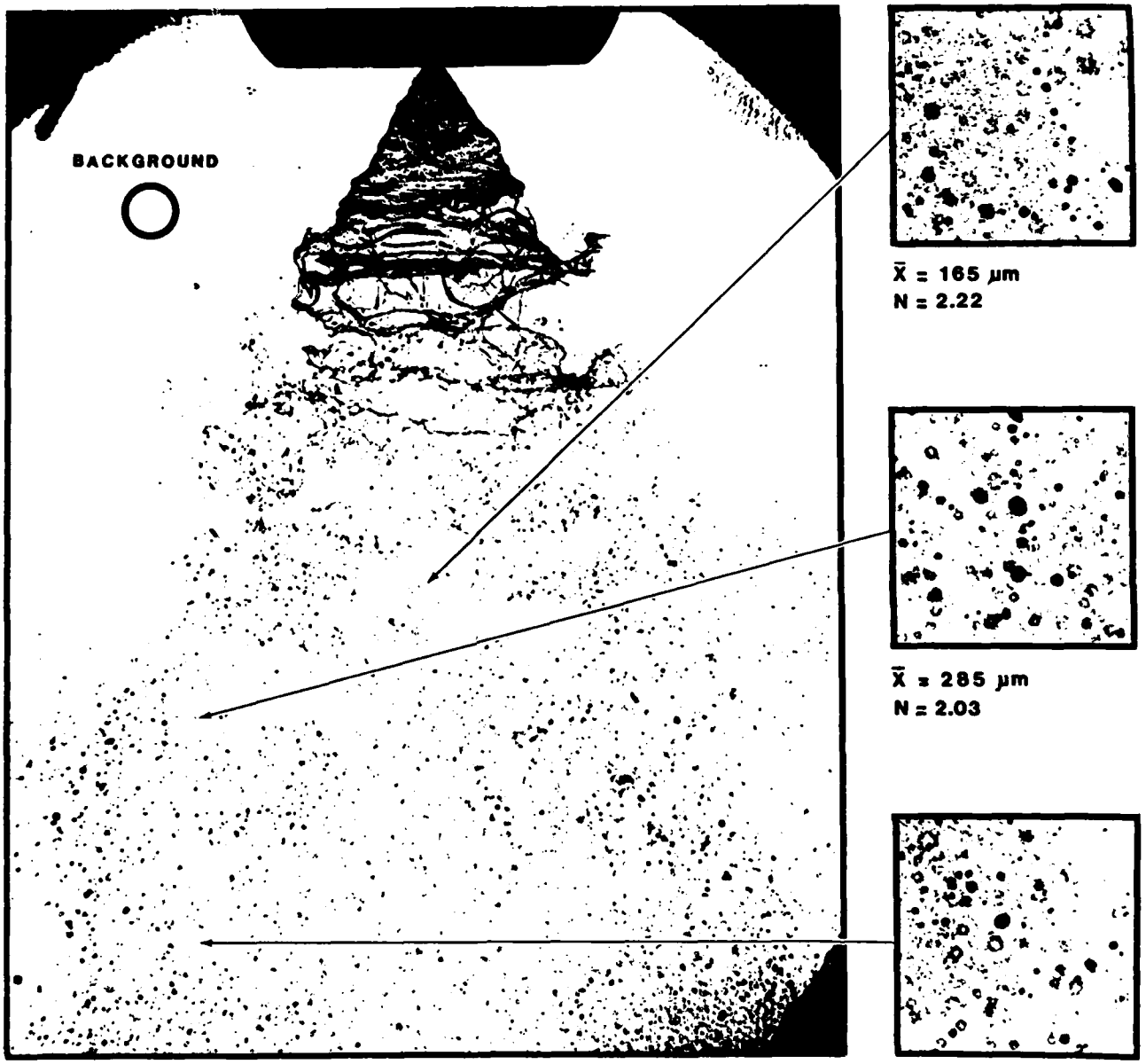

FUEL : SRC 2
NOZZLE : SIMPLEX
CONDITIONS : 100 PSI, 75°F
PRE-MAGNIFICATION OF SPRAY HOLOGRAM : 3X
$\bar{X}$,N : PARAMETERS OF ROSSIN RAMMLER DISTRIBUTION

Figure 13.

6.0 FUTURE WORK

The goal of the next phase of this work will be to produce and demonstrate a prototype recording and data reduction system with integrated holographic and Fourier transform analysis systems.

The results of Phase I have demonstrated the feasibility of this technique under ideal controlled conditions as well as an actual spray hologram. The approach under Phase II will be to demonstrate the data reduction capabilities in an extended range of environments of interest to the Department of Defense (DoD) and obtain data which until now have been unattainable.

Due to the success experienced with the Malvern receiver during Phase I and the fact that many government agencies and private industries already have such instrument, it is attractive to consider it for the Fourier diffraction analysis. On the other hand, the Malvern system was designed for real time data acquisition and may not be optimal for the proposed application. The ideal Fourier transform analyzer will be defined and its features will be compared to the Malvern receiver.

For the most part, the approach will be to develop the best holographic interface to the Malvern receiver and to test it, demonstrate it, and acquire unique and needed data.

The objectives are two-fold: (1) to produce the best possible holograms and reconstruct them as faithfully as possible minimizing the noise while optimizing the signal; (2) to use the most adequate Fourier transform analyzer of the scattered radiation.

The results obtained under Phase I indicate the areas that require improvements. These areas are:

(a) Increase the diffraction efficiency by using phase holograms. This should have a positive effect on the S/N. We expect a ten-fold increase in the efficiency.

(b) Reduce the holographic noise by minimizing extraneous light and scattering agents on the surface of the plate.

(c) Use plate holders which will allow repositioning the hologram with extreme accuracy (such as double plate holographic interferometer plate holder).

(d) Consider thermoplastic emulsions in a single data acquisition/reconstruction system to avoid moving the hologram as well as to provide rapid, on-line results.

(e) Explore the feasibility of constructing and reconstructing with the same wavelength to eliminate achromatic errors. The limitation here is imposed by the need of pulse lasers. YAG lasers can provide such source of illumination and possibly recontruction. Another approach could be constructing the hologram with the YAG laser with a wavelength of 5320Å and reconstructing it with a Krypton ion laser at 5309Å, or an Argon ion laser at 5287Å.

(f) Using the more conventional Ruby for construction and HeNe for reconstruction, correct the change in wavelength of the size parameter.

Upon development of a holographic construction-reconstruction-Fourier analysis system, the approach will be to test and demonstrate it in various environments of interest. In order of complexity they are:

(1) Steady State Sprays. This will allow direct comparison between the hologram and the spray. Note that Fourier transform analyzing the light scattered by an unsteady spray will result in a time average which is different than the distribution found at any arbitrary time. It is, therefore, necessary to produce a steady spray in order to obtain good agreement.

(2) Unsteady Sprays. This can be accomplished with a variable pressure drive thus resulting in a changing and cyclic size and velocity distributions. Holograms can be obtained at selected times, synchronized with the driving mechanism and thus resolve the time evolving size distribution.

(3) Burning Sprays. A simple kerosene burning spray can be used in these experiments. Here the proposed system will provide capabilities not yet achieved. Scattering instruments are limited in hot environments because of the

refraction imposed on the laser. The laser beam will wander as the result of this fluctuating refraction, therefore impairing on the alignment. Laser pulse holography will freeze the action and analyses can be conducted afterwards with the Fourier diffraction analyzer.

(4) Transverse Injector in a Cross Flow at the Kamjet Fuel Injection Facility at Wright-Patterson. This demonstration will be extremely significant since it combines the requirements and difficulties of the previous ones. Laser pulse holography should prove very powerful when obtaining measurements in the combustor. If steady state conditions can be achieved, the results can then be compared to those obtained directly with the Malvern.

7.0 REFERENCES

1. B. C. R. Ewan, "Fraunhofer Plane Analysis of Particle Field Holograms", Applied Optics, Vol. 19, No. 8, 1980.

APPENDIX 1

MALVERN OUTPUT DATA

MALVERN 2600/3600 PARTICLE SIZER VF.3

MALVERN INSTRUMENTS LTD, SPRING LANE, MALVERN, ENGLAND.

PRINTING PARAMETERS

RUN NO.	TIME	MODEL	X BAR	N	LOG ERROR
12	20-57-30	ROS-RAM	43.19	3.05	5.14

PRINTING RESULTS FROM DATA BLOCK 1

SAMPLE CONCENTRATION = 0.0000% BY VOLUME OBSCURATION = 1.00

SIZE BAND UPPER	LOWER	CUMULATIVE WT BELOW	WEIGHT IN BAND	CUMULATIVE % WT ABOVE
320	310	100.0	0.0	0.0
310	300	100.0	0.0	0.0
300	290	100.0	0.0	0.0
290	280	100.0	0.0	0.0
280	270	100.0	0.0	0.0
270	260	100.0	0.0	0.0
260	250	100.0	0.0	0.0
250	240	100.0	0.0	0.0
240	230	100.0	0.0	0.0
230	220	100.0	0.0	0.0
220	210	100.0	0.0	0.0
210	200	100.0	0.0	0.0
200	190	100.0	0.0	0.0
190	180	100.0	0.0	0.0
180	170	100.0	0.0	0.0
170	160	100.0	0.0	0.0
160	150	100.0	0.0	0.0
150	140	100.0	0.0	0.0
140	130	100.0	0.0	0.0
130	120	100.0	0.0	0.0
120	110	100.0	0.0	0.0
110	100	100.0	0.0	0.0
100	90	99.9	0.1	0.0
90	80	99.1	0.8	0.1
80	70	95.6	3.5	0.9
70	60	85.8	9.8	4.4
60	50	67.3	18.5	14.2
50	40	43.2	24.1	32.7
40	30	21.0	22.3	56.8
30	20	6.6	14.4	79.0
20	10	0.8	5.8	93.4
10	0	0.0	0.8	99.2

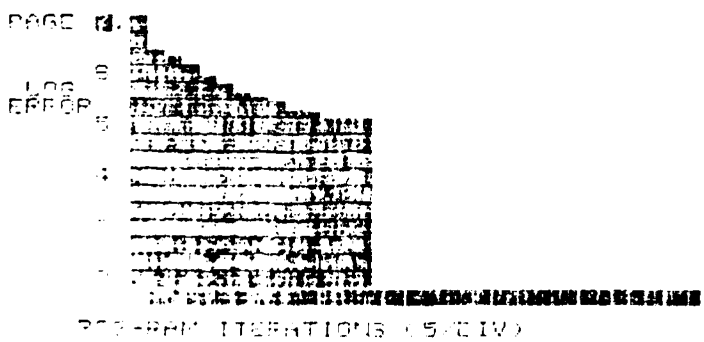

Figure 1. Size histogram of hologram 12 (I_o = .094 mw) with hologram 13 (I_o = .105 mw) as background. Rossin Rammler software. Receiver was aligned to background only.

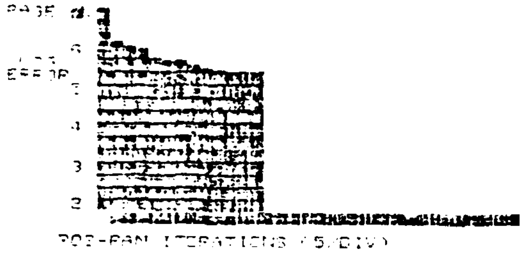

MALVERN 2600/3600 PARTICLE SIZER VF.3

MALVERN INSTRUMENTS LTD.SPRING LANE,MALVERN,ENGLAND.

PRINTING PARAMETERS

RUN NO.	TIME	MODEL	X BAR	N	LOG ERROR
113	15-52-10	ROS-RAM	47.40	2.56	5.53

PRINTING RESULTS FROM DATA BLOCK 12

SAMPLE CONCENTRATION = 0.0000% BY VOLUME   OBSCURATION = 1.00

SIZE BAND UPPER	LOWER	CUMULATIVE WT BELOW	WEIGHT IN BAND	CUMULATIVE % WT ABOVE
320	310	100.0	0.0	0.0
310	300	100.0	0.0	0.0
300	290	100.0	0.0	0.0
290	280	100.0	0.0	0.0
280	270	100.0	0.0	0.0
270	260	100.0	0.0	0.0
260	250	100.0	0.0	0.0
250	240	100.0	0.0	0.0
240	230	100.0	0.0	0.0
230	220	100.0	0.0	0.0
220	210	100.0	0.0	0.0
210	200	100.0	0.0	0.0
200	190	100.0	0.0	0.0
190	180	100.0	0.0	0.0
180	170	100.0	0.0	0.0
170	160	100.0	0.0	0.0
160	150	100.0	0.0	0.0
150	140	100.0	0.0	0.0
140	130	100.0	0.0	0.0
130	120	100.0	0.0	0.0
120	110	100.0	0.0	0.0
110	100	[illegible]	[illegible]	0.0
100	90	[illegible]	0.4	[illegible]
90	80	[illegible]	1.6	0.5
80	70	[illegible]	4.4	2.1
70	60	[illegible]	9.4	6.5
60	50	[illegible]	15.[illegible]	[illegible]
50	40	47.[illegible]	20.[illegible]	31.[illegible]
40	30	26.[illegible]	21.[illegible]	[illegible]
30	20	10.[illegible]	16.[illegible]	[illegible]
20	10	1.[illegible]	[illegible]	[illegible]
10	0	[illegible]	1.0	[illegible].2

PRINTING DATA BLOCK 12

RUN NO.	TIME	OBSCURATION
113	15-52-10	1.00

INDEX	DATA
1	- 6.41
2	- 1.13
3	- 0.89
4	- 0.34
5	0.06
6	0.34
7	[illegible]
8	1.03
9	1.55
10	2.00
11	2.44
[illegible]	2.66
[illegible]	1.34
[illegible]	2.41
[illegible]	[illegible]
[illegible]	[illegible]
[illegible]	3.12
[illegible]	3.0[illegible]
[illegible]	3.0[illegible]
[illegible]	[illegible]
[illegible]	[illegible]
[illegible]	[illegible]
[illegible]	[illegible]
[illegible]	[illegible]
[illegible]	[illegible]
[illegible]	[illegible]
[illegible]	[illegible]
[illegible]	[illegible]
[illegible]	[illegible]
[illegible]	[illegible]

Figure 2. Repeat of size histogram of hologram 12 with hologram 13 as background. Receiver was aligned to background only.

MALVERN 2600/3600 PARTICLE SIZER VF.3

MALVERN INSTRUMENTS LTD, SPRING LANE, MALVERN, ENGLAND.

PRINTING PARAMETERS

RUN NO.	TIME	MODEL	M BAR	N	LOG ERROR
146	16-13-10	POS-RAM	45.23	3.30	5.60

PRINTING RESULTS FROM DATA BLOCK 3

SAMPLE CONCENTRATION = 0.0437% BY VOLUME OBSCURATION = 0.40

SIZE BAND UPPER	LOWER	CUMULATIVE WT BELOW	WEIGHT IN BAND	CUMULATIVE % WT ABOVE
320	310	100.0	0.0	0.0
310	300	100.0	0.0	0.0
300	290	100.0	0.0	0.0
290	280	100.0	0.0	0.0
280	270	100.0	0.0	0.0
270	260	100.0	0.0	0.0
260	250	100.0	0.0	0.0
250	240	100.0	0.0	0.0
240	230	100.0	0.0	0.0
230	220	100.0	0.0	0.0
220	210	100.0	0.0	0.0
210	200	100.0	0.0	0.0
200	190	100.0	0.0	0.0
190	180	100.0	0.0	0.0
180	170	100.0	0.0	0.0
170	160	100.0	0.0	0.0
160	150	100.0	0.0	0.0
150	140	100.0	0.0	0.0
140	130	100.0	0.0	0.0
130	120	100.0	0.0	0.0
120	110	100.0	0.0	0.0
110	100	100.0	0.0	0.0
100	90	100.0	0.0	0.0
90	80	100.0	0.0	0.0
80	70	99.5	0.5	0.5
70	60	94.5	4.5	5.4
60	50	76.6	17.9	23.4
50	40	46.5	30.3	53.4
40	30	19.0	27.6	81.0
30	20	4.4	14.6	95.6
20	10	0.3	4.1	99.[illegible]
10	0	0.0	0.3	[illegible]

PRINTING DATA BLOCK 3

RUN NO.	TIME	OBSCURATION
146	16-13-10	0.40

INDEX	DATA
1	- 5.01
2	- [illegible]
3	0.8[illegible]
4	[illegible].1[illegible]
5	0.1[illegible]
6	0.44
7	[illegible].7[illegible]
8	1.[illegible]
9	[illegible]
10	[illegible]
11	[illegible]
12	2.31
13	[illegible]
14	3.06
15	3.74
16	4.13
17	[illegible].20
18	[illegible].74
19	3.[illegible]
20	2.59
21	2.47
22	2.16
23	1.97
24	1.73
25	1.62
26	1.5[illegible]
27	1.5[illegible]
28	1.[illegible]
29	1.1[illegible]
30	0.34

Figure 3. Repeat of size histogram of hologram 12 with hologram 13 as background. Receiver was aligned to background and also to signal.

MALVERN 2600/3600 PARTICLE SIZER VF.3

MALVERN INSTRUMENTS LTD SPRING LANE,MALVERN,ENGLAND.

PRINTING PARAMETERS

RUN NO.	TIME	MODEL	F.F	N	LOG ERROR
3	09-44-40	ROS-RAM	31.14	3.36	5.82

PRINTING RESULTS FROM DATA BLOCK 1

SAMPLE CONCENTRATION = 0.0264% BY VOLUME OBSCURATION = 0.23

SIZE BAND UPPER	SIZE BAND LOWER	CUMULATIVE WT BELOW	WEIGHT IN BAND	CUMULATIVE % WT ABOVE
320	310	100.0	0.0	0.0
310	300	100.0	0.0	0.0
300	290	100.0	0.0	0.0
290	280	100.0	0.0	0.0
280	270	100.0	0.0	0.0
270	260	100.0	0.0	0.0
260	250	100.0	0.0	0.0
250	240	100.0	0.0	0.0
240	230	100.0	0.0	0.0
230	220	100.0	0.0	0.0
220	210	100.0	0.0	0.0
210	200	100.0	0.0	0.0
200	190	100.0	0.0	0.0
190	180	100.0	0.0	0.0
180	170	100.0	0.0	0.0
170	160	100.0	0.0	0.0
160	150	100.0	0.0	0.0
150	140	100.0	0.0	0.0
140	130	100.0	0.0	0.0
130	120	100.0	0.0	0.0
120	110	100.0	0.0	0.0
110	100	100.0	0.0	0.0
100	90	100.0	0.0	0.0
90	80	99.5	0.5	0.0
80	70	95.6	3.9	[illegible]
70	60	82.2	[illegible]	4.4
60	50	57.[illegible]	[illegible]	17.8
50	40	[illegible]	[illegible]	42.7
40	30	11.1	13.0	68.9
30	20	2.4	8.7	88.9
20	10	0.8	2.2	97.6
10	[illegible]	0.0	0.2	99.8

Figure 4. Size histogram of hologram 21 (I_o = .14 mw) with hologram 20 (I_o = .15 mw) as background. Data were obtained first thing in the morning without realigning the Malvern.

MALVERN 2600/3600 PARTICLE SIZER VF.3

MALVERN INSTRUMENTS LTD,SPRING LANE,MALVERN,ENGLAND.

PRINTING PARAMETERS

RUN NO.	TIME	MODEL	X BAR	N	LOG ERROR
13	[illegible]	[illegible]-RAM	31.47	3.78	5.68

PRINTING RESULTS FROM DATA BLOCK 2

SAMPLE CONCENTRATION = 0.0070% BY VOLUME OBSCURATION = 0.32

SIZE BAND UPPER	SIZE BAND LOWER	CUMULATIVE WT BELOW	WEIGHT IN BAND	CUMULATIVE % WT ABOVE
320	310	100.0	0.0	0.0
310	300	100.0	0.0	0.0
300	290	100.0	0.0	0.0
290	280	100.0	0.0	0.0
280	270	100.0	0.0	0.0
270	260	100.0	0.0	0.0
260	250	100.0	0.0	0.0
250	240	100.0	0.0	0.0
240	230	100.0	0.0	0.0
230	220	100.0	0.0	0.0
220	210	100.0	0.0	0.0
210	200	100.0	0.0	0.0
200	190	100.0	0.0	0.0
190	180	100.0	0.0	0.0
180	170	100.0	0.0	0.0
170	160	100.0	0.0	0.0
160	150	100.0	0.0	0.0
150	140	100.0	0.0	0.0
140	130	100.0	0.0	0.0
130	120	100.0	0.0	0.0
120	110	100.0	0.0	0.0
110	100	100.0	0.0	0.0
100	90	100.0	0.0	0.0
90	80	99.4	0.6	0.0
80	70	95.6	3.8	0.6
70	60	82.9	12.7	4.4
60	50	59.3	23.6	17.1
50	40	32.5	26.8	40.7
40	30	12.7	19.8	67.5
30	20	3.0	9.7	87.3
20	10	0.3	2.7	97.0
10	0	0.0	0.2	99.8

Figure 5. Repeat of size histogram of hologram 21 with hologram 20 as background after minor receiver realignment.

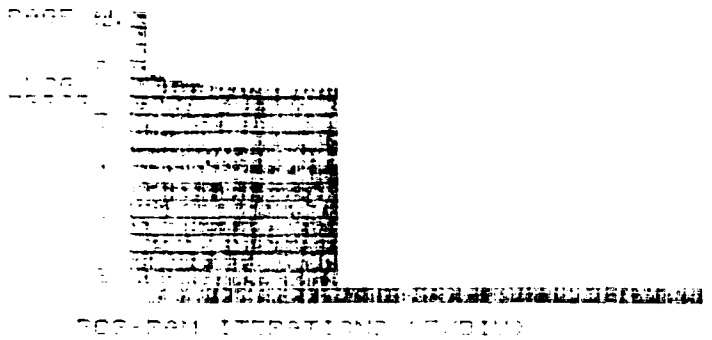

MALVERN 2600/3600 PARTICLE SIZER VF.3

MALVERN INSTRUMENTS LTD.SPRING LANE,MALVERN,ENGLAND.

PRINTING PARAMETERS

RUN NO.	TIME	MODEL	% BAD	n	LOG ERROR
20	23-FEB-88	POST-RRI	30.31	3.7±	5.63

PRINTING RESULTS FROM DATA BLOCK 4

SAMPLE CONCENTRATION = 0.0313% BY VOLUME OBSCURATION = 6.20

SIZE BAND UPPER	SIZE BAND LOWER	PERCENTAGE OUT BELOW	WEIGHT IN BAND	CUMULATIVE % WT ABOVE

Figure 6a. Size histogram of hologram 21 with hologram 20 as background. Rossin Rammler software. Corresponds to Figure 10 (Text).

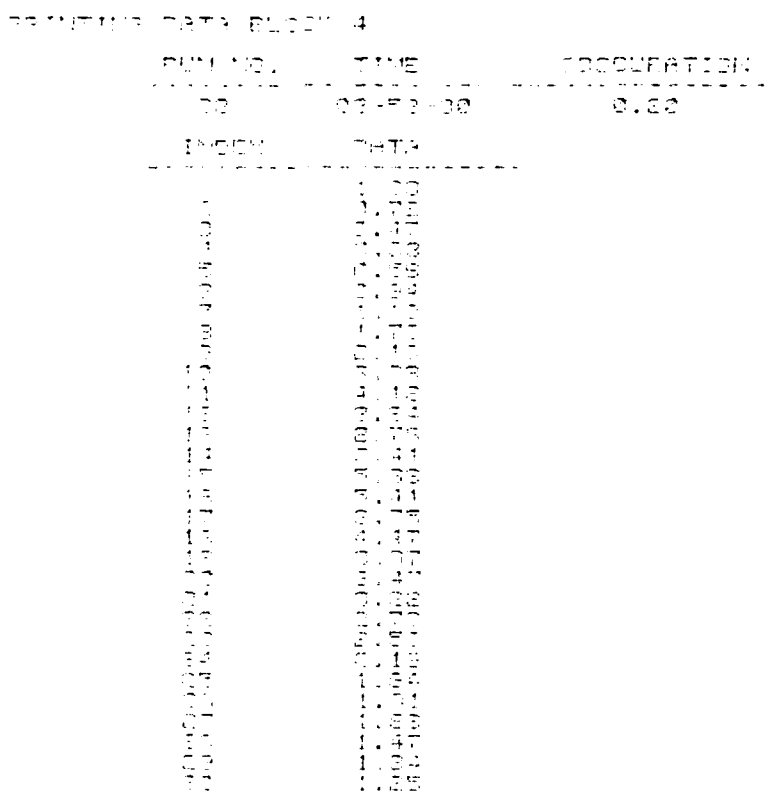

Figure 6b. Volts per diode corresponding to Figure 6a and Figure 10 (Text).

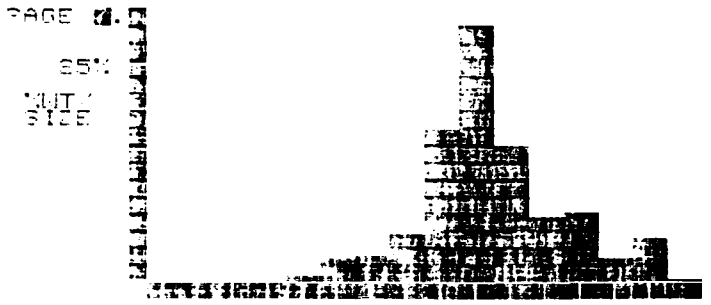

MALVERN 2600/3600 PARTICLE SIZER VF.3

MALVERN INSTRUMENTS LTD,SPRING LANE,MALVERN,ENGLAND.

PRINTING RESULTS FROM DATA BLOCK 6

TIME 11-19-40 RUN NO. 10 LOG ERROR = 4.50

SAMPLE CONCENTRATION = 0.0123 % BY VOLUME
OBSCURATION = 0.11

SIZE BAND UPPER	SIZE BAND LOWER	CUMULATIVE WT BELOW	WEIGHT IN BAND	CUMULATIVE WT ABOVE	LIGHT ENERGY COMPUTED	LIGHT ENERGY MEASURED
564.0	261.8	99.5	0.5	0.0	197	155
261.8	190.4	94.4	5.2	0.5	325	353
190.4	112.8	91.4	3.0	5.6	474	438
112.8	84.3	83.3	8.1	8.6	667	686
84.3	64.6	76.0	7.3	16.7	956	938
64.6	50.2	60.5	15.5	24.0	1324	1282
50.2	39.0	30.3	30.2	39.5	1745	1770
39.0	30.3	12.6	17.7	69.7	2047	2047
30.3	23.7	7.2	5.4	87.4	2032	1954
23.7	18.5	4.1	3.0	92.8	1609	1563
18.5	14.5	1.6	2.9	95.6	1164	1241
14.5	11.4	0.3	0.9	98.6	1061	982
11.4	9.1	0.1	0.2	99.7	905	770
9.1	7.2	0.0	0.1	99.8	623	621
7.2	5.8	0.0	0.0	100.0	480	493

Figure 7. Size histogram of directly measured photomask with glass substrate as background. Model independent software. I_o = 0.5 mw illustrates effect of not focusing unscattered light on center diode.

MALVERN 2600/3600 PARTICLE SIZER VF.3

MALVERN INSTRUMENTS LTD,SPRING LANE,MALVERN,ENGLAND.

PRINTING PARAMETERS

RUN NO.	TIME	MODEL	X BAR	N	LOG ERROR
37	10-05-20	ROS-RAM	50.64	3.33	3.35

PRINTING RESULTS FROM DATA BLOCK 10

SAMPLE CONCENTRATION = 0.0130% BY VOLUME OBSCURATION = 0.13

SIZE BAND UPPER	SIZE BAND LOWER	CUMULATIVE WT BELOW	WEIGHT IN BAND	CUMULATIVE % WT ABOVE
220	210	100.0	0.0	0.0
210	200	100.0	0.0	0.0
200	190	100.0	0.0	0.0
190	180	100.0	0.0	0.0
180	170	100.0	0.0	0.0
170	160	100.0	0.0	0.0
160	150	100.0	0.0	0.0
150	140	100.0	0.0	0.0
140	130	100.0	0.0	0.0
130	120	100.0	0.0	0.0
120	110	100.0	0.0	0.0
110	100	100.0	0.0	0.0
100	90	99.9	0.1	0.0
90	80	99.1	0.8	0.1
80	70	95.0	4.1	0.9
70	60	83.1	11.9	5.0
60	50	61.6	21.4	16.9
50	40	36.2	25.4	38.4
40	30	15.6	20.6	63.8
30	20	4.2	11.4	84.4
20	10	0.4	3.6	95.8
10	0	0.0	0.4	99.6

PAGE 1.

ROS-RAM ITERATIONS (5/DIV)

Figure 8. Rossin Rammler parameters corresponding to Figure 11 (Text).

MALVERN 2600/3600 PARTICLE SIZER VF.3

MALVERN INSTRUMENTS LTD,SPRING LANE,MALVERN,ENGLAND.

PRINTING PARAMETERS

RUN NO.	TIME	MODEL	X BAR	N	LOG ERROR
39	10-41-40	ROS-RAM	50.64	3.36	3.72

PRINTING RESULTS FROM DATA BLOCK 11

SAMPLE CONCENTRATION = 0.0125% BY VOLUME   OBSCURATION = 0.13

SIZE BAND UPPER	SIZE BAND LOWER	CUMULATIVE WT BELOW	WEIGHT IN BAND	CUMULATIVE % WT ABOVE
320	310	100.0	0.0	0.0
310	300	100.0	0.0	0.0
300	290	100.0	0.0	0.0
290	280	100.0	0.0	0.0
280	270	100.0	0.0	0.0
270	260	100.0	0.0	0.0
260	250	100.0	0.0	0.0
250	240	100.0	0.0	0.0
240	230	100.0	0.0	0.0
230	220	100.0	0.0	0.0
220	210	100.0	0.0	0.0
210	200	100.0	0.0	0.0
200	190	100.0	0.0	0.0
190	180	100.0	0.0	0.0
180	170	100.0	0.0	0.0
170	160	100.0	0.0	0.0
160	150	100.0	0.0	0.0
150	140	100.0	0.0	0.0
140	130	100.0	0.0	0.0
130	120	100.0	0.0	0.0
120	110	100.0	0.0	0.0
110	100	100.0	0.0	0.0
100	90	99.9	0.1	0.0
90	80	99.1	0.8	0.1

Figure 9. Rossin Rammler parameters corresponding to Figure 12 (Text).

MALVERN 2600/3600 PARTICLE SIZER VF.3

MALVERN INSTRUMENTS LTD,SPRING LANE,MALVERN,ENGLAND.

PRINTING PARAMETERS

RUN NO.	TIME	MODEL	X BAR	N	LOG ERROR
19	10-56-30	ROS-RAM	284.59	2.03	5.83

PRINTING RESULTS FROM DATA BLOCK 1

SAMPLE CONCENTRATION = 0.0474% BY VOLUME OBSCURATION = 0.11

SIZE BAND UPPER	SIZE BAND LOWER	CUMULATIVE UT BELOW	WEIGHT IN BAND	CUMULATIVE % WT ABOVE
[illegible]	[illegible]	[illegible]	[illegible]	[illegible]

PAGE [illegible]

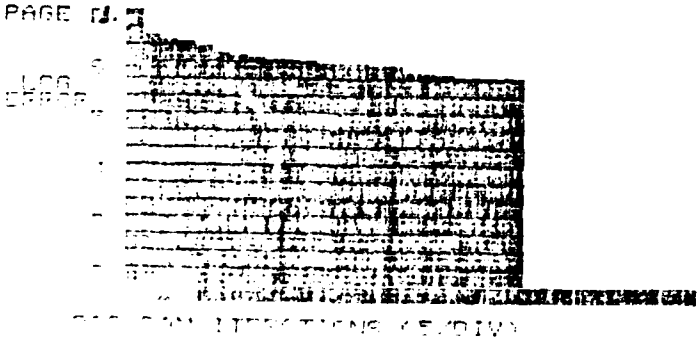

Figure 10a. Size histogram of spray hologram obtained with Rossin Rammler software. Corresponds to center view of Figure 13 (Text).

PRINTING DATA BLOCK 1

RUN NO.	TIME	OBSCURATION
19	10-56-30	0.11

INDEX	DATA
1	11.41
2	10.69
3	11.69
4	0.77
5	0.41
6	0.16
7	0.00
8	0.00
9	0.00
10	0.00
11	0.00
12	0.00
13	0.00
14	0.00
15	0.00
16	0.00
17	0.00
18	0.00
19	0.00
20	0.00
21	0.00
22	0.00
23	0.00
24	0.00
25	0.00
26	0.00
27	0.00
28	0.00
29	0.00
30	0.00
31	0.00
32	0.00
33	0.00
34	0.00
35	0.00
36	0.00
37	0.00
38	0.00
39	0.00
40	0.00

Figure 10b. Volts per ring corresponding to Figure 10a.

MALVERN 2600/3600 PARTICLE SIZER VF.3

MALVERN INSTRUMENTS LTD, SPRING LANE, MALVERN, ENGLAND.

PRINTING PARAMETERS

RUN NO.	TIME	MODEL	% BAR	U	LOG ERROR
80	11-05-00	2OB-RAM	277.35	2.06	5.33

PRINTING RESULTS FROM DATA BLOCK 2

SAMPLE CONCENTRATION = 0.0541% BY VOLUME OBSCURATION = 0.13

SIZE BAND UPPER	SIZE BAND LOWER	CUMULATIVE WT BELOW	WEIGHT IN BAND	CUMULATIVE % WT ABOVE
880	710	100.0	0.3	0.0
710	560	99.7	0.4	0.3
560	440	99.3	0.6	0.7
440	350	98.7	1.0	1.3
350	280	97.7	1.4	2.3
280	220	96.3	1.8	3.7
220	180	94.5	2.2	5.5
180	140	92.3	2.6	7.7
140	110	89.7	2.9	10.3
110	88	86.8	3.1	13.2
88	70	83.7	3.3	16.3
70	56	80.4	3.4	19.6
56	44	77.0	3.4	23.0
44	35	73.6	3.4	26.4
35	28	70.2	3.3	29.8
28	22	66.9	3.2	33.1
22	18	63.7	3.0	36.3
18	14	60.7	2.8	39.3
14	11	57.9	2.6	42.1
11	8.8	55.3	2.4	44.7
8.8	7.0	52.9	2.2	47.1
7.0	5.6	50.7	2.0	49.3
5.6	4.4	48.7	1.8	51.3
4.4	3.5	46.9	1.6	53.1
3.5	2.8	45.3	1.5	54.7
2.8	2.2	43.8	1.3	56.2
2.2	1.8	42.5	1.2	57.5
1.8	1.4	41.3	1.1	58.7
1.4	1.1	40.2	1.0	59.8
1.1	0.88	39.2	0.9	60.8
0.88	0.70	38.3	0.8	61.7
0.70	0.56	37.5	0.7	62.5
0.56	0.44	36.8	0.7	63.2
0.44	0.35	36.1	0.6	63.9
0.35	0.28	35.5	0.6	64.5
0.28	0.22	34.9	0.5	65.1
0.22	0.18	34.4	0.5	65.6
0.18	0.14	33.9	0.4	66.1
0.14	0.11	33.5	0.4	66.5
0.11	0.088	33.1	0.4	66.9
0.088	0.070	32.7	0.3	67.3
0.070	0.056	32.4	0.3	67.6
0.056	0.044	32.1	0.3	67.9
0.044	0.035	31.8	0.3	68.2
0.035	0.028	31.5	0.2	68.5
0.028	0.022	31.3	0.2	68.7
0.022	0.018	31.1	0.2	68.9
0.018	0.014	30.9	0.2	69.1
0.014	0.011	30.7	0.2	69.3
0.011	0.0088	30.5	0.1	69.5
0.0088	0.0070	30.4	0.1	69.6
0.0070	0.0056	30.3	0.1	69.7
0.0056	0.0044	30.2	0.1	69.8
0.0044	0.0035	30.1	0.1	69.9
0.0035	0.0028	30.0	0.1	70.0
0.0028	0.0022	29.9	0.1	70.1
0.0022	0.0018	29.8	0.1	70.2
0.0018	0.0014	29.7	0.1	70.3
0.0014	0.0011	29.6	0.1	70.4
0.0011	0.00088	29.5	0.1	70.5
0.00088	0.00070	29.4	0.1	70.6
0.00070	0.00056	29.3	0.1	70.7
0.00056	0.00044	29.2	0.1	70.8
0.00044	0.00035	29.1	0.1	70.9
0.00035	0.00028	29.0	0.1	71.0
0.00028	0.00022	28.9	0.1	71.1
0.00022	0.00018	28.8	0.1	71.2
0.00018	0.00014	28.7	0.1	71.3
0.00014	0.00011	28.6	0.1	71.4
0.00011	0.000088	28.5	0.1	71.5
0.000088	0.000070	28.4	0.1	71.6
0.000070	0.000056	28.3	0.1	71.7
0.000056	0.000044	28.2	0.1	71.8
0.000044	0.000035	28.1	0.1	71.9
0.000035	0.000028	28.0	0.1	72.0
0.000028	0.000022	27.9	0.1	72.1
0.000022	0.000018	27.8	0.1	72.2
0.000018	0.000014	27.7	0.1	72.3
0.000014	0.000011	27.6	0.1	72.4
0.000011	0.0000088	27.5	0.1	72.5
0.0000088	0.0000070	27.4	0.1	72.6
0.0000070	0.0000056	27.3	0.1	72.7
0.0000056	0.0000044	27.2	0.1	72.8
0.0000044	0.0000035	27.1	0.1	72.9
0.0000035	0.0000028	27.0	0.1	73.0
0.0000028	0.0000022	26.9	0.1	73.1
0.0000022	0.0000018	26.8	0.1	73.2
0.0000018	0.0000014	26.7	0.1	73.3
0.0000014	0.0000011	26.6	0.1	73.4
0.0000011	0.00000088	26.5	0.1	73.5
0.00000088	0.00000070	26.4	0.1	73.6
0.00000070	0.00000056	26.3	0.1	73.7
0.00000056	0.00000044	26.2	0.1	73.8
0.00000044	0.00000035	26.1	0.1	73.9
0.00000035	0.00000028	26.0	0.1	74.0
0.00000028	0.00000022	25.9	0.1	74.1
0.00000022	0.00000018	25.8	0.1	74.2
0.00000018	0.00000014	25.7	0.1	74.3
0.00000014	0.00000011	25.6	0.1	74.4
0.00000011	0.000000088	25.5	0.1	74.5
0.000000088	0.000000070	25.4	0.1	74.6
0.000000070	0.000000056	25.3	0.1	74.7
0.000000056	0.000000044	25.2	0.1	74.8
0.000000044	0.000000035	25.1	0.1	74.9
0.000000035	0.000000028	25.0	0.1	75.0
0.000000028	0.000000022	24.9	0.1	75.1
0.000000022	0.000000018	24.8	0.1	75.2
0.000000018	0.000000014	24.7	0.1	75.3
0.000000014	0.000000011	24.6	0.1	75.4
0.000000011	0.0000000088	24.5	0.1	75.5
0.0000000088	0.0000000070	24.4	0.1	75.6
0.0000000070	0.0000000056	24.3	0.1	75.7
0.0000000056	0.0000000044	24.2	0.1	75.8
0.0000000044	0.0000000035	24.1	0.1	75.9
0.0000000035	0.0000000028	24.0	0.1	76.0
0.0000000028	0.0000000022	23.9	0.1	76.1
0.0000000022	0.0000000018	23.8	0.1	76.2
0.0000000018	0.0000000014	23.7	0.1	76.3
0.0000000014	0.0000000011	23.6	0.1	76.4
0.0000000011	0.00000000088	23.5	0.1	76.5
0.00000000088	0.00000000070	23.4	0.1	76.6
0.00000000070	0.00000000056	23.3	0.1	76.7
0.00000000056	0.00000000044	23.2	0.1	76.8
0.00000000044	0.00000000035	23.1	0.1	76.9
0.00000000035	0.00000000028	23.0	0.1	77.0
0.00000000028	0.00000000022	22.9	0.1	77.1
0.00000000022	0.00000000018	22.8	0.1	77.2
0.00000000018	0.00000000014	22.7	0.1	77.3
0.00000000014	0.00000000011	22.6	0.1	77.4
0.00000000011	0.000000000088	22.5	0.1	77.5
0.000000000088	0.000000000070	22.4	0.1	77.6
0.000000000070	0.000000000056	22.3	0.1	77.7
0.000000000056	0.000000000044	22.2	0.1	77.8
0.000000000044	0.000000000035	22.1	0.1	77.9
0.000000000035	0.000000000028	22.0	0.1	78.0
0.000000000028	0.000000000022	21.9	0.1	78.1
0.000000000022	0.000000000018	21.8	0.1	78.2
0.000000000018	0.000000000014	21.7	0.1	78.3
0.000000000014	0.000000000011	21.6	0.1	78.4
0.000000000011	0.0000000000088	21.5	0.1	78.5
0.0000000000088	0.0000000000070	21.4	0.1	78.6
0.0000000000070	0.0000000000056	21.3	0.1	78.7
0.0000000000056	0.0000000000044	21.2	0.1	78.8
0.0000000000044	0.0000000000035	21.1	0.1	78.9
0.0000000000035	0.0000000000028	21.0	0.1	79.0
0.0000000000028	0.0000000000022	20.9	0.1	79.1
0.0000000000022	0.0000000000018	20.8	0.1	79.2
0.0000000000018	0.0000000000014	20.7	0.1	79.3
0.0000000000014	0.0000000000011	20.6	0.1	79.4
0.0000000000011	0.00000000000088	20.5	0.1	79.5
0.00000000000088	0.00000000000070	20.4	0.1	79.6
0.00000000000070	0.00000000000056	20.3	0.1	79.7
0.00000000000056	0.00000000000044	20.2	0.1	79.8
0.00000000000044	0.00000000000035	20.1	0.1	79.9
0.00000000000035	0.00000000000028	20.0	0.1	80.0
0.00000000000028	0.00000000000022	19.9	0.1	80.1
0.00000000000022	0.00000000000018	19.8	0.1	80.2
0.00000000000018	0.00000000000014	19.7	0.1	80.3
0.00000000000014	0.00000000000011	19.6	0.1	80.4
0.00000000000011	0.000000000000088	19.5	0.1	80.5
0.000000000000088	0.000000000000070	19.4	0.1	80.6
0.000000000000070	0.000000000000056	19.3	0.1	80.7
0.000000000000056	0.000000000000044	19.2	0.1	80.8
0.000000000000044	0.000000000000035	19.1	0.1	80.9
0.000000000000035	0.000000000000028	19.0	0.1	81.0
0.000000000000028	0.000000000000022	18.9	0.1	81.1
0.000000000000022	0.000000000000018	18.8	0.1	81.2
0.000000000000018	0.000000000000014	18.7	0.1	81.3
0.000000000000014	0.000000000000011	18.6	0.1	81.4
0.000000000000011	0.0000000000000088	18.5	0.1	81.5
0.0000000000000088	0.0000000000000070	18.4	0.1	81.6
0.0000000000000070	0.0000000000000056	18.3	0.1	81.7
0.0000000000000056	0.0000000000000044	18.2	0.1	81.8
0.0000000000000044	0.0000000000000035	18.1	0.1	81.9
0.0000000000000035	0.0000000000000028	18.0	0.1	82.0
0.0000000000000028	0.0000000000000022	17.9	0.1	82.1
0.0000000000000022	0.0000000000000018	17.8	0.1	82.2
0.0000000000000018	0.0000000000000014	17.7	0.1	82.3
0.0000000000000014	0.0000000000000011	17.6	0.1	82.4
0.0000000000000011	0.00000000000000088	17.5	0.1	82.5
0.00000000000000088	0.00000000000000070	17.4	0.1	82.6
0.00000000000000070	0.00000000000000056	17.3	0.1	82.7
0.00000000000000056	0.00000000000000044	17.2	0.1	82.8
0.00000000000000044	0.00000000000000035	17.1	0.1	82.9
0.00000000000000035	0.00000000000000028	17.0	0.1	83.0
0.00000000000000028	0.00000000000000022	16.9	0.1	83.1
0.00000000000000022	0.00000000000000018	16.8	0.1	83.2
0.00000000000000018	0.00000000000000014	16.7	0.1	83.3
0.00000000000000014	0.00000000000000011	16.6	0.1	83.4
0.00000000000000011	0.000000000000000088	16.5	0.1	83.5
0.000000000000000088	0.000000000000000070	16.4	0.1	83.6
0.000000000000000070	0.000000000000000056	16.3	0.1	83.7
0.000000000000000056	0.000000000000000044	16.2	0.1	83.8
0.000000000000000044	0.000000000000000035	16.1	0.1	83.9
0.000000000000000035	0.000000000000000028	16.0	0.1	84.0
0.000000000000000028	0.000000000000000022	15.9	0.1	84.1
0.000000000000000022	0.000000000000000018	15.8	0.1	84.2
0.000000000000000018	0.000000000000000014	15.7	0.1	84.3
0.000000000000000014	0.000000000000000011	15.6	0.1	84.4
0.000000000000000011	0.0000000000000000088	15.5	0.1	84.5
0.0000000000000000088	0.0000000000000000070	15.4	0.1	84.6
0.0000000000000000070	0.0000000000000000056	15.3	0.1	84.7
0.0000000000000000056	0.0000000000000000044	15.2	0.1	84.8
0.0000000000000000044	0.0000000000000000035	15.1	0.1	84.9
0.0000000000000000035	0.0000000000000000028	15.0	0.1	85.0
0.0000000000000000028	0.0000000000000000022	14.9	0.1	85.1
0.0000000000000000022	0.0000000000000000018	14.8	0.1	85.2
0.0000000000000000018	0.0000000000000000014	14.7	0.1	85.3
0.0000000000000000014	0.0000000000000000011	14.6	0.1	85.4
0.0000000000000000011	0.00000000000000000088	14.5	0.1	85.5
0.00000000000000000088	0.00000000000000000070	14.4	0.1	85.6
0.00000000000000000070	0.00000000000000000056	14.3	0.1	85.7
0.00000000000000000056	0.00000000000000000044	14.2	0.1	85.8
0.00000000000000000044	0.00000000000000000035	14.1	0.1	85.9
0.00000000000000000035	0.00000000000000000028	14.0	0.1	86.0
0.00000000000000000028	0.00000000000000000022	13.9	0.1	86.1
0.00000000000000000022	0.00000000000000000018	13.8	0.1	86.2
0.00000000000000000018	0.00000000000000000014	13.7	0.1	86.3
0.00000000000000000014	0.00000000000000000011	13.6	0.1	86.4
0.00000000000000000011	0.000000000000000000088	13.5	0.1	86.5
0.000000000000000000088	0.000000000000000000070	13.4	0.1	86.6
0.000000000000000000070	0.000000000000000000056	13.3	0.1	86.7
0.000000000000000000056	0.000000000000000000044	13.2	0.1	86.8
0.000000000000000000044	0.000000000000000000035	13.1	0.1	86.9
0.000000000000000000035	0.000000000000000000028	13.0	0.1	87.0
0.000000000000000000028	0.000000000000000000022	12.9	0.1	87.1
0.000000000000000000022	0.000000000000000000018	12.8	0.1	87.2
0.000000000000000000018	0.000000000000000000014	12.7	0.1	87.3
0.000000000000000000014	0.000000000000000000011	12.6	0.1	87.4
0.000000000000000000011	0.0000000000000000000088	12.5	0.1	87.5
0.0000000000000000000088	0.0000000000000000000070	12.4	0.1	87.6
0.0000000000000000000070	0.0000000000000000000056	12.3	0.1	87.7
0.0000000000000000000056	0.0000000000000000000044	12.2	0.1	87.8
0.0000000000000000000044	0.0000000000000000000035	12.1	0.1	87.9
0.0000000000000000000035	0.0000000000000000000028	12.0	0.1	88.0
0.0000000000000000000028	0.0000000000000000000022	11.9	0.1	88.1
0.0000000000000000000022	0.0000000000000000000018	11.8	0.1	88.2
0.0000000000000000000018	0.0000000000000000000014	11.7	0.1	88.3
0.0000000000000000000014	0.0000000000000000000011	11.6	0.1	88.4
0.0000000000000000000011	0.00000000000000000000088	11.5	0.1	88.5
0.00000000000000000000088	0.00000000000000000000070	11.4	0.1	88.6
0.00000000000000000000070	0.00000000000000000000056	11.3	0.1	88.7
0.00000000000000000000056	0.00000000000000000000044	11.2	0.1	88.8
0.00000000000000000000044	0.00000000000000000000035	11.1	0.1	88.9
0.00000000000000000000035	0.00000000000000000000028	11.0	0.1	89.0
0.00000000000000000000028	0.00000000000000000000022	10.9	0.1	89.1
0.00000000000000000000022	0.00000000000000000000018	10.8	0.1	89.2
0.00000000000000000000018	0.00000000000000000000014	10.7	0.1	89.3
0.00000000000000000000014	0.00000000000000000000011	10.6	0.1	89.4
0.00000000000000000000011	0.000000000000000000000088	10.5	0.1	89.5
0.000000000000000000000088	0.000000000000000000000070	10.4	0.1	89.6
0.000000000000000000000070	0.000000000000000000000056	10.3	0.1	89.7
0.000000000000000000000056	0.000000000000000000000044	10.2	0.1	89.8
0.000000000000000000000044	0.000000000000000000000035	10.1	0.1	89.9
0.000000000000000000000035	0.000000000000000000000028	10.0	0.1	90.0
0.000000000000000000000028	0.000000000000000000000022	9.9	0.1	90.1
0.000000000000000000000022	0.000000000000000000000018	9.8	0.1	90.2
0.000000000000000000000018	0.000000000000000000000014	9.7	0.1	90.3
0.000000000000000000000014	0.000000000000000000000011	9.6	0.1	90.4
0.000000000000000000000011	0.0000000000000000000000088	9.5	0.1	90.5
0.0000000000000000000000088	0.0000000000000000000000070	9.4	0.1	90.6
0.0000000000000000000000070	0.0000000000000000000000056	9.3	0.1	90.7
0.0000000000000000000000056	0.0000000000000000000000044	9.2	0.1	90.8
0.0000000000000000000000044	0.0000000000000000000000035	9.1	0.1	90.9
0.0000000000000000000000035	0.0000000000000000000000028	9.0	0.1	91.0
0.0000000000000000000000028	0.0000000000000000000000022	8.9	0.1	91.1
0.0000000000000000000000022	0.0000000000000000000000018	8.8	0.1	91.2
0.0000000000000000000000018	0.0000000000000000000000014	8.7	0.1	91.3
0.0000000000000000000000014	0.0000000000000000000000011	8.6	0.1	91.4
0.0000000000000000000000011	0.00000000000000000000000088	8.5	0.1	91.5
0.00000000000000000000000088	0.00000000000000000000000070	8.4	0.1	91.6
0.00000000000000000000000070	0.00000000000000000000000056	8.3	0.1	91.7
0.00000000000000000000000056	0.00000000000000000000000044	8.2	0.1	91.8
0.00000000000000000000000044	0.00000000000000000000000035	8.1	0.1	91.9
0.00000000000000000000000035	0.00000000000000000000000028	8.0	0.1	92.0
0.00000000000000000000000028	0.00000000000000000000000022	7.9	0.1	92.1
0.00000000000000000000000022	0.00000000000000000000000018	7.8	0.1	92.2
0.00000000000000000000000018	0.00000000000000000000000014	7.7	0.1	92.3
0.00000000000000000000000014	0.00000000000000000000000011	7.6	0.1	92.4
0.00000000000000000000000011	0.000000000000000000000000088	7.5	0.1	92.5
0.000000000000000000000000088	0.000000000000000000000000070	7.4	0.1	92.6
0.000000000000000000000000070	0.000000000000000000000000056	7.3	0.1	92.7
0.000000000000000000000000056	0.000000000000000000000000044	7.2	0.1	92.8
0.000000000000000000000000044	0.000000000000000000000000035	7.1	0.1	92.9
0.000000000000000000000000035	0.000000000000000000000000028	7.0	0.1	93.0
0.000000000000000000000000028	0.000000000000000000000000022	6.9	0.1	93.1
0.000000000000000000000000022	0.000000000000000000000000018	6.8	0.1	93.2
0.000000000000000000000000018	0.000000000000000000000000014	6.7	0.1	93.3
0.000000000000000000000000014	0.000000000000000000000000011	6.6	0.1	93.4
0.000000000000000000000000011	0.0000000000000000000000000088	6.5	0.1	93.5
0.0000000000000000000000000088	0.0000000000000000000000000070	6.4	0.1	93.6
0.0000000000000000000000000070	0.0000000000000000000000000056	6.3	0.1	93.7
0.0000000000000000000000000056	0.0000000000000000000000000044	6.2	0.1	93.8
0.0000000000000000000000000044	0.0000000000000000000000000035	6.1	0.1	93.9
0.0000000000000000000000000035	0.0000000000000000000000000028	6.0	0.1	94.0
0.0000000000000000000000000028	0.0000000000000000000000000022	5.9	0.1	94.1
0.0000000000000000000000000022	0.0000000000000000000000000018	5.8	0.1	94.2
0.0000000000000000000000000018	0.0000000000000000000000000014	5.7	0.1	94.3
0.0000000000000000000000000014	0.0000000000000000000000000011	5.6	0.1	94.4
0.0000000000000000000000000011	0.00000000000000000000000000088	5.5	0.1	94.5
0.00000000000000000000000000088	0.00000000000000000000000000070	5.4	0.1	94.6
0.00000000000000000000000000070	0.00000000000000000000000000056	5.3	0.1	94.7
0.00000000000000000000000000056	0.00000000000000000000000000044	5.2	0.1	94.8
0.00000000000000000000000000044	0.00000000000000000000000000035	5.1	0.1	94.9
0.00000000000000000000000000035	0.00000000000000000000000000028	5.0	0.1	95.0
0.00000000000000000000000000028	0.00000000000000000000000000022	4.9	0.1	95.1
0.00000000000000000000000000022	0.00000000000000000000000000018	4.8	0.1	95.2
0.00000000000000000000000000018	0.00000000000000000000000000014	4.7	0.1	95.3
0.00000000000000000000000000014	0.00000000000000000000000000011	4.6	0.1	95.4
0.00000000000000000000000000011	0.000000000000000000000000000088	4.5	0.1	95.5
0.000000000000000000000000000088	0.000000000000000000000000000070	4.4	0.1	95.6
0.000000000000000000000000000070	0.000000000000000000000000000056	4.3	0.1	95.7
0.000000000000000000000000000056	0.000000000000000000000000000044	4.2	0.1	95.8
0.000000000000000000000000000044	0.000000000000000000000000000035	4.1	0.1	95.9
0.000000000000000000000000000035	0.000000000000000000000000000028	4.0	0.1	96.0
0.000000000000000000000000000028	0.000000000000000000000000000022	3.9	0.1	96.1
0.000000000000000000000000000022	0.000000000000000000000000000018	3.8	0.1	96.2
0.000000000000000000000000000018	0.000000000000000000000000000014	3.7	0.1	96.3
0.000000000000000000000000000014	0.000000000000000000000000000011	3.6	0.1	96.4
0.000000000000000000000000000011	0.0000000000000000000000000000088	3.5	0.1	96.5
0.0000000000000000000000000000088	0.0000000000000000000000000000070	3.4	0.1	96.6
0.0000000000000000000000000000070	0.0000000000000000000000000000056	3.3	0.1	96.7
0.0000000000000000000000000000056	0.0000000000000000000000000000044	3.2	0.1	96.8
0.0000000000000000000000000000044	0.0000000000000000000000000000035	3.1	0.1	96.9
0.0000000000000000000000000000035	0.0000000000000000000000000000028	3.0	0.1	97.0
0.0000000000000000000000000000028	0.0000000000000000000000000000022	2.9	0.1	97.1
0.0000000000000000000000000000022	0.0000000000000000000000000000018	2.8	0.1	97.2
0.0000000000000000000000000000018	0.0000000000000000000000000000014	2.7	0.1	97.3
0.0000000000000000000000000000014	0.0000000000000000000000000000011	2.6	0.1	97.4
0.0000000000000000000000000000011	0.00000000000000000000000000000088	2.5	0.1	97.5
0.00000000000000000000000000000088	0.00000000000000000000000000000070	2.4	0.1	97.6
0.00000000000000000000000000000070	0.00000000000000000000000000000056	2.3	0.1	97.7
0.00000000000000000000000000000056	0.00000000000000000000000000000044	2.2	0.1	97.8
0.00000000000000000000000000000044	0.00000000000000000000000000000035	2.1	0.1	97.9
0.00000000000000000000000000000035	0.00000000000000000000000000000028	2.0	0.1	98.0
0.00000000000000000000000000000028	0.00000000000000000000000000000022	1.9	0.1	98.1
0.00000000000000000000000000000022	0.00000000000000000000000000000018	1.8	0.1	98.2
0.00000000000000000000000000000018	0.00000000000000000000000000000014	1.7	0.1	98.3
0.00000000000000000000000000000014	0.00000000000000000000000000000011	1.6	0.1	98.4
0.00000000000000000000000000000011	0.000000000000000000000000000000088	1.5	0.1	98.5
0.000000000000000000000000000000088	0.000000000000000000000000000000070	1.4	0.1	98.6
0.000000000000000000000000000000070	0.000000000000000000000000000000056	1.3	0.1	98.7
0.000000000000000000000000000000056	0.000000000000000000000000000000044	1.2	0.1	98.8
0.000000000000000000000000000000044	0.000000000000000000000000000000035	1.1	0.1	98.9
0.000000000000000000000000000000035	0.000000000000000000000000000000028	1.0	0.1	99.0
0.000000000000000000000000000000028	0.000000000000000000000000000000022	0.9	0.1	99.1
0.000000000000000000000000000000022	0.000000000000000000000000000000018	0.8	0.1	99.2
0.000000000000000000000000000000018	0.000000000000000000000000000000014	0.7	0.1	99.3
0.000000000000000000000000000000014	0.000000000000000000000000000000011	0.6	0.1	99.4
0.000000000000000000000000000000011	0.0000000000000000000000000000000088	0.5	0.1	99.5
0.0000000000000000000000000000000088	0.0000000000000000000000000000000070	0.4	0.1	99.6
0.0000000000000000000000000000000070	0.0000000000000000000000000000000056	0.3	0.1	99.7
0.0000000000000000000000000000000056	0.0000000000000000000000000000000044	0.2	0.1	99.8
0.0000000000000000000000000000000044	0.0000000000000000000000000000000035	0.1	0.1	99.9
0.0000000000000000000000000000000035	0.0000000000000000000000000000000028	0.0	0.1	100.0

PAGE 1.

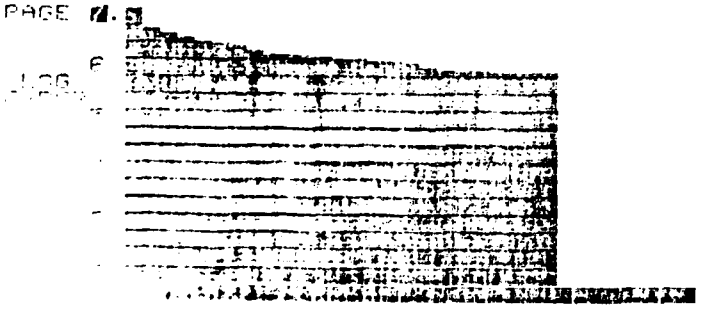

FOR ITERATIONS (5/DIV)

Figure 11a. Repeat of position shown on Figure 10a.

PRINTING DATA BLOCK 2

RUN NO.	TIME	OBSCURATION
20	11-05-[illegible]	0.13

INDEX	DATA
1	[illegible]
[illegible]	[illegible]
[illegible]	[illegible]
4	[illegible]
[illegible]	[illegible]
[illegible]	[illegible]
[illegible]	[illegible]
[illegible]	[illegible]
[illegible]	[illegible]
[illegible]	[illegible]
[illegible]	[illegible]
[illegible]	[illegible]
[illegible]	[illegible]
[illegible]	5.38
[illegible]	4.81
[illegible]	3.31
[illegible]	[illegible]
[illegible]	3.81
[illegible]	3.53
[illegible]	3.94
[illegible]	4.34
[illegible]	4.84
[illegible]	3.75
[illegible]	2.28
[illegible]	0.84
[illegible]	0.03
[illegible]	- 0.34
[illegible]	- 0.19
[illegible]	- 0.31
30	- 0.34

Figure 11b. Volts per ring corresponding to Figure 11a.

MALVERN 3600D/3600E PARTICLE SIZER VF.3

MALVERN INSTRUMENTS LTD,SPRING LANE,MALVERN,ENGLAND.

PRINTING PARAMETERS

RUN NO.	TIME	MODEL	X BAR	N	LOG ERROR
34	11:50:00	300-RAM	253.63	2.57	5.63

PRINTING RESULTS FROM DATA BLOCK 3

SAMPLE CONCENTRATION = 0.0381% BY VOLUME OBSCURATION = 0.19

SIZE BAND UPPER	SIZE BAND LOWER	CUMULATIVE WT BELOW	WEIGHT IN BAND	CUMULATIVE % WT ABOVE
720	310	78.0	2.7	19.3
310	300	75.2	3.3	22.0
300	290	72.1	3.1	24.9
290	280	69.0	3.2	27.8
280	270	65.4	3.4	31.1
270	260	61.8	3.6	34.5
260	250	58.2	3.6	38.1
250	240	54.4	3.8	41.8
240	230	50.4	3.9	45.6
230	220	46.5	3.9	49.5
220	210	42.6	3.9	53.4
210	200	38.7	3.9	57.3
200	190	35.1	3.6	61.0
190	180	31.5	3.6	64.6
180	170	28.1	3.4	68.0
170	160	24.8	3.3	71.3
160	150	21.8	3.0	74.3
150	140	19.1	2.7	77.1
140	130	16.7	2.4	79.6
130	120	14.6	2.1	81.7
120	110	12.7	1.9	83.6
110	100	11.0	1.7	85.3
100	90	9.5	1.5	86.8
90	80	8.2	1.3	88.1
80	70	7.0	1.2	89.3
70	60	6.0	1.0	90.3
60	50	5.1	0.9	91.2
50	40	4.3	0.8	92.0
40	30	3.6	0.7	92.7
30	20	2.9	0.7	93.4
20	15	2.4	0.5	94.0
15	10	1.9	0.5	94.5
10	9	1.7	0.2	94.7
9	8	1.5	0.2	94.9
8	7	1.3	0.2	95.1
7	6	1.1	0.2	95.3
6	5	0.9	0.2	95.5
5	4	0.7	0.2	95.7
4	3	0.5	0.2	95.9
3	2	0.3	0.2	96.1
2	1	0.1	0.2	96.3
1	0	0.0	0.1	96.5

PAGE 1.

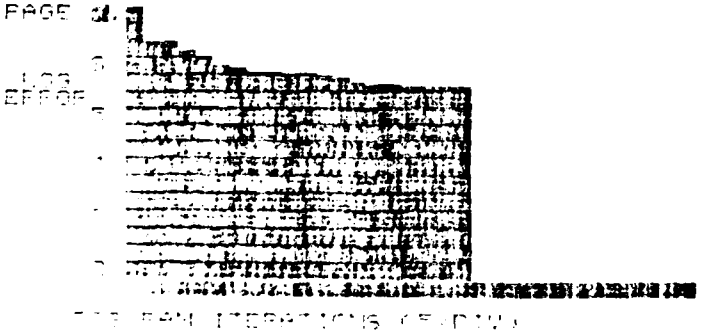

RAM ITERATIONS (F.D.V.)

Figure 12a. Size histogram of spray hologram obtained with Rossin Rammler software. Corresponds to lower view of Figure 13 (Text).

PRINTING DATA BLOCK 2

RUN NO.	TIME	OBSCURATION
24	11-00-00	0.19

INDEX	DATA
1	11.50
2	0.56
3	0.00
4	0.00
5	0.00
6	0.00
7	0.00
8	0.00
9	0.00
10	0.00
11	0.00
12	0.00
13	0.00
14	0.00
15	0.00
16	0.00
17	0.00
18	0.00
19	0.00
20	1.34
21	1.06
22	0.00
23	0.00
24	0.00
25	0.00
26	0.00
27	0.00
28	0.00
29	0.19
30	0.00

Figure 12b. Volts per ring corresponding to Figure 12a.

MALVERN 3300/3600 PARTICLE SIZER VF.3

MALVERN INSTRUMENTS LTD.SPRING LANE,MALVERN,ENGLAND.

PRINTING PARAMETERS

RUN NO.	TIME	MODEL	X PAR	N	LOG ERROR
37	11-26-10	POS-RAM	184.83	2.32	3.78

PRINTING RESULTS FROM DATA BLOCK 4

SAMPLE CONCENTRATION = 0.026% BY VOLUME OBSCURATION = 0.32

SIZE BAND UPPER	SIZE BAND LOWER	CUMULATIVE WT BELOW	WEIGHT IN BAND	CUMULATIVE % WT ABOVE
1000.0	816	98.6	0.4	1.4
816	666	98.2	0.4	1.8
666	543	97.8	0.8	2.2
543	443	97.0	1.4	3.0
443	362	95.6	1.4	4.4
362	295	94.2	1.8	5.8
295	241	92.4	2.0	7.6
241	196	90.4	2.0	9.6
196	160	88.4	2.0	11.6
160	131	86.4	2.0	13.6
131	106	84.4	2.0	15.6
106	87.0	82.4	2.0	17.6
87.0	71.0	80.4	2.0	19.6
71.0	58.0	78.4	2.0	21.6
58.0	47.4	76.4	2.0	23.6
47.4	38.7	74.4	2.0	25.6
38.7	31.6	72.4	2.0	27.6
31.6	25.8	70.4	2.0	29.6
25.8	21.1	68.4	2.0	31.6
21.1	17.2	66.4	2.0	33.6
17.2	14.1	64.4	2.0	35.6
14.1	11.5	62.4	2.0	37.6
11.5	9.40	60.4	2.0	39.6
9.40	7.68	58.4	2.0	41.6
7.68	6.27	56.4	2.0	43.6
6.27	5.12	54.4	2.0	45.6
5.12	4.18	52.4	2.0	47.6
4.18	3.42	50.4	2.0	49.6
3.42	2.79	48.4	2.0	51.6
2.79	2.28	46.4	2.0	53.6
2.28	1.86	44.4	2.0	55.6
1.86	1.52	42.4	2.0	57.6
1.52	1.24	40.4	2.0	59.6
1.24	1.01	38.4	2.0	61.6
1.01	0.827	36.4	2.0	63.6
0.827	0.675	34.4	2.0	65.6
0.675	0.552	32.4	2.0	67.6
0.552	0.450	30.4	2.0	69.6
0.450	0.368	28.4	2.0	71.6
0.368	0.300	26.4	2.0	73.6
0.300	0.245	24.4	2.0	75.6
0.245	0.200	22.4	2.0	77.6
0.200	0.163	20.4	2.0	79.6
0.163	0.133	18.4	2.0	81.6
0.133	0.109	16.4	2.0	83.6
0.109	0.089	14.4	2.0	85.6
0.089	0.072	12.4	2.0	87.6
0.072	0.059	10.4	2.0	89.6
0.059	0.048	8.40	2.0	91.6
0.048	0.039	6.40	2.0	93.6
0.039	0.032	4.40	2.0	95.6
0.032	0.026	2.40	2.0	97.6
0.026	0.021	0.40	2.0	99.6

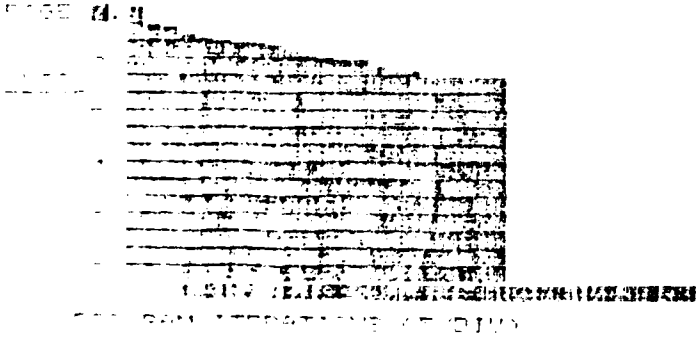

Figure 13a. Size histogram of spray hologram obtained with Rossin Rammler software. Corresponds to upper detail view of Figure 13 (Text).

PRINTING DATA BLOCK 4

RUN NO.	TIME	OBSERVATION
27	11-33-30	0.38

INDEX	DATA
1	0.0
2	0.0
3	0.0
4	0.0
5	0.0
6	0.0
7	0.0
8	0.0
9	0.0
10	0.0
11	0.0
12	0.0
13	0.0
14	0.0
15	0.0
16	0.0
17	0.0
18	0.0
19	0.0
20	0.0
21	0.0
22	0.0
23	0.0
24	0.0
25	0.0
26	0.0
27	0.0
28	0.0
29	0.0
30	0.0
31	0.0
32	0.0
33	0.0
34	0.0
35	0.0
36	0.0
37	0.0
38	0.0
39	0.0
40	0.0
41	0.0
42	0.0
43	0.0
44	0.0
45	0.0
46	0.0
47	0.0
48	0.0
49	0.0
50	0.0
51	0.0
52	0.0
53	0.0
54	0.0
55	0.0
56	0.0
57	0.0
58	0.0
59	0.0
60	0.0

Figure 13b. Volts per ring corresponding to Figure 13a.

APPENDIX 2

HOLOGRAM PROCESSING, OPTIMIZATION, AND CHARACTERIZATION

APPENDIX 2

1.0 HOLOGRAM PROCESSING, OPTIMIZATION, AND CHARACTERIZATION

1.1 Hologram Quality

The quality of a hologram can be defined by three parameters: (1) diffraction efficiency (brightness), defined as the ratio of the diffracted (or reconstructed) and illuminating (or reconstructing) energy levels, (2) resolution (spatial bandwidth) and, (3) signal-to-noise ratio (the smallest retrievable object intensity).

Diffraction efficiency depends upon the type of emulsion and upon holographic fringe visibility. Fringe visibility is highest when the object and reference waves are of equal intensity. (This is not where the highest signal-to-noise occurs). In some material diffraction efficiency can approach 100 percent resulting in extremely bright holograms. Brightness is an important parameter for some applications and it becomes important in particle diagnostic applications when light detector thresholds are approached. A direct tradeoff occurs between reconstruction laser power, detector sensitivity, and hologram diffraction efficiency.

Resolution is defined by recording geometry, hologram size, emulsion type, and the quality of optical components. Optical component quality can be compensated for by proper recording and reconstruction procedures.

Signal-to-noise ratio (S/N) is defined by the type of emulsion and by the overall quality of procedure, for example, cleanliness, linear recording, use of liquid gates, and refined processing methods.

Therefore, in producing a hologram one must pay attention to four things which can be mutually excluding and requiring tradeoff.

(1) Maximum diffraction efficiency for a bright image
(2) High S/N for a clean image
(3) High resolution for good image definition
(4) A short recording time so that motion during recording is not a factor.

1.2 Noise Sources

Optical noise is probably the most limiting parameter in particle holography. Coherent noise appearing in the form of speckle causes images to break up into small patches of light which are difficult to distinguish from signal. This reduces the true resolution of the recording. Also, coherent noise can render virtually any automated image analyzer unusable.

In this discussion any light which is not a part of the immediate image under examination will be considered noise. The following are noise sources. (Refer to Figure 1 and Table I).

1. The beam emerging from the laser does not have a smooth intensity profile. This can be caused by dirty laser windows, laser misalignment, laser design.
2. The object beam, upon striking the hologram contains light which has been scattered from the original laser beam by scatterers

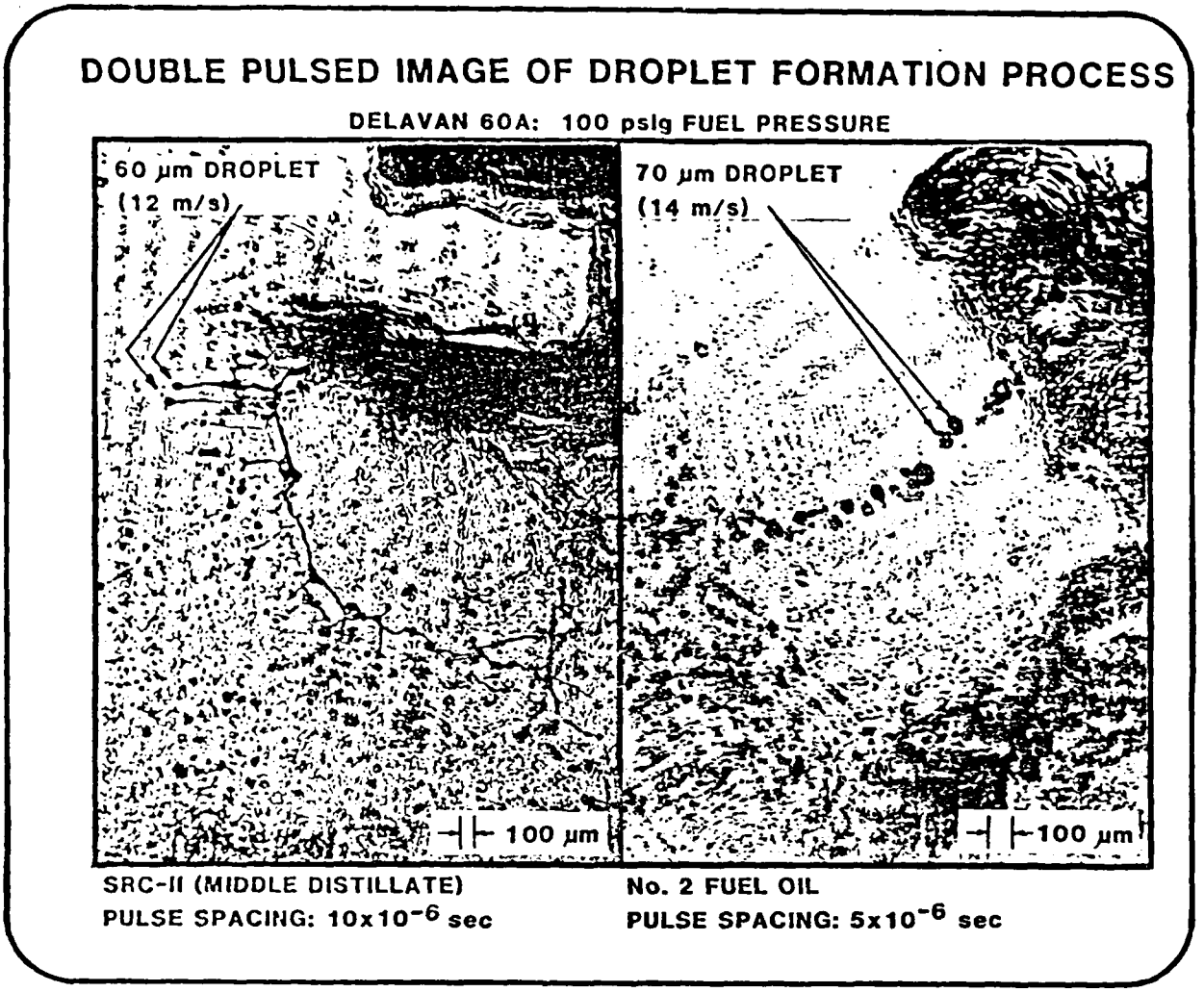

82-1586P-10

Figure 1.

TABLE 1

- COHERENT NOISE EVIDENT IN ABOVE PICTURES
  - Film Grain Noise
  - Contaminant Diffraction Patterns
  - Interference of Emulsion Surfaces
  - Interference of Substrate Surfaces
  - Out-of-Focus Images

other than the object field. There may be contaminants on optical surfaces or anywhere else, scratches, surface texture of components.

3. The reference beam contains light scattered from the original laser beam by contaminants, scratches, or surface texture of components.

4. Either object or reference waves may contain additional wavefronts caused by multiple reflection in beamsplitters, lenses, the recording emulsion, and the emulsion backing. These give rise to multiple images and interference fringes which cause nonuniform recording intensity.

5. Nonlinear recording creates a noise component which is predicted through holography theory. This component of noise is negligible when the exposure range on the emulsion remains in a region wherein the amplitude transmittance is proportional to exposure. A recording can be recognized as nonlinear through the multiplicity and brightness of reconstruction orders beyond the first.

6. Scattering by the emulsion grain creates a speckle noise which increases with emulsion density as well as with development time.

7. Diffraction noise from edges is impossible to avoid entirely. A diffraction pattern in the object or reference wave causes a density variation in the hologram. This makes it impossible to optimize exposure and the diffraction pattern intensity variation reappears in the reconstructed image.

8. Light scattered from contaminants in the reconstruction system optics as well as in the hologram appear in the reconstructed image.

9. Light scattered from the part of the object field not under immediate observation into the region of observation can be highly limiting. This occurs in large volumes and in high number

density particle field studies when plane-by-plane observation is desired. It is not a factor, however, when an integrated light scattering measurement is desired.

10. A hologram is made by mixing an object wave with a reference wave. In fact, the hologram does not distinguish waves. On the same recording holograms are made by the interference of object and noise source waves, noise source and reference wave, and by light coming from different parts of the object wave. Reduction of the latter noise source can be reduced only by optimizing recording geometry and this will be discussed further.

Unlike incoherent light, scattered or reflected coherent light interferes with the signal causing much larger intensity variations. For example, a secondary beam having intensity of only 1 percent of the main beam will contain fringes of about 20 percent contrast! Therefore, contamination and secondary reflections are more serious from a noise standpoint in coherent optics.

A major task of successful holography is the choice of recording geometry, components and processing technique to minimize the noise sources listed above.

1.3 Real Emulsion Characteristics

Emulsion characteristics which must be considered are resolution, modulation transfer function (MTF), contrast (Gamma), sensitivity and noise. An extremely useful collection of tables describing various holographic emulson characteristics can be found in reference 2. Certain parts of those tables have been extracted and presented here.

The typical behavior of a holographic emulsion is summarized in Figure 2, which describes a generic holography film.

As the exposure increases, the diffraction efficiency (proportional to α^2) increases until it peaks at a density of approximately 0.8 (for all holography emulsions) after which it decreases as the exposure increases further. The grain noise, likewise, first increases with exposure, peaks (before the diffraction efficiency has peaked) then decreases as the effect of added density is to reduce the amount of light transmitted by the emulsion at a rate exceeding the increase in amount of light scattered by the grain.

Note that the grain noise is heavily peaked in the direction of the illuminating beam. This suggests that one should choose as large an angle between object and reference waves as is possible until some other effect becomes important.

Reference 2 summarizes the necessary constants for five different emulsions which can be used to quantify image quality.

1.4 Computing Signal to Noise Ratio

Reconstructed image intensity is given by $I_{rec}\eta$ where η is the diffraction efficiency at the hologram and I_{rec} is the reconstructing wave intensity

$$\eta = \left[22\ \alpha(\bar{E}) \cdot m\ (\nu) \cdot M\ (\nu)\right]^2 \sim \alpha^2$$

$$\text{where} \quad \alpha(\bar{E}) = \left(\frac{dT_a}{d\ \log\ E}\right)_{\bar{E}} = \frac{-\ell n 10}{2}\ \tau_a\ (\bar{E}) \cdot v\ (\bar{E}) \qquad (1)$$

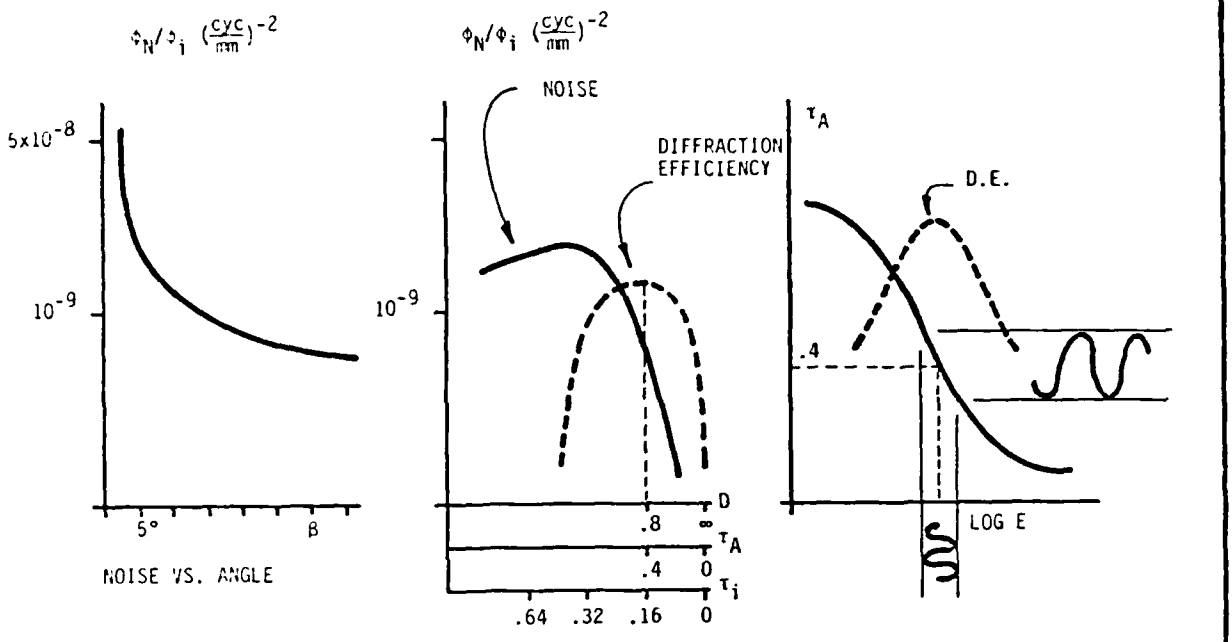

Figure 2.

CHARACTERISTICS OF SILVER HALIDE EMULSIONS

DEFINITIONS:

Φ_N - Optical noise power reconstructed per bandwidth squared

Φ_i - Incident optical flux

β - Angle between incident light and the measured quantity

D - Photographic density

τ_A - Amplitude transmission coefficient

τ_i - Intensity transmission coefficient

E Exposure

D.E. - Diffraction efficiency

84-2338-03A-2

$m(\nu) \sim$ input modulation $\Delta(\log E)$

$M(\nu) \sim$ modulation transfer function

$\nu \sim$ recording spatial frequency

$\gamma \sim$ film gamma

$$I_{rec} = I_{ref}\eta = I_{ref}\left[.22\ \alpha m \gamma\right]^2 \qquad (2)$$

letting $\alpha^2 = 3$, $M = .6$ and $I_R > I_O$ (Typical values)

$$I_{rec} - I_{ref}\ (.05)\ \log\left[\frac{E_R + 2\sqrt{E_R E_h}}{E_R - 2\sqrt{E_R E_h}}\right]$$

$E_R \sim$ reference wave exposure

$E_h \sim$ object wave illumination which actually strikes the hologram.

Assuming the scatter cross section is the actual cross section, the exposure at the hologram, E_h, arising from the object is

$$E_h = \frac{d^2 R}{4\left(1.22\ \frac{s\lambda}{d}\right)^2}$$

$$= \frac{0.168\ d^4 R E_o}{s^2 \lambda^2}$$

where S is the object-hologram distance

R is the scatter coefficient

d is the element diameter in the object field.

$$\frac{I_{rec}}{I_{noise}} = \frac{.05}{\phi_N B^2} \log \left[\frac{E_R + 2\sqrt{E_r E_h}}{E_R - 2\sqrt{E_r E_h}} \right] = \frac{.05}{\phi_N B^2} \log \left[\frac{1 + 2\sqrt{\frac{E_h}{E_r}}}{1 - 2\sqrt{\frac{E_h}{E_r}}} \right] \qquad (3)$$

where B = required bandwidth cycles/mm

E_R = reference exposure

E_h = object illumination reaching the hologram

$$= \frac{d^4 R}{4\pi^2 \lambda^2 S^2} E_O$$

d = element diameter

R = reflection coefficient

λ = wavelength

S = distance object to hologram

Figure 3 is a plot of Equation 3 for a typical emulsion.

1.5 Optimizing Film Exposure and Processing

To achieve the best quality hologram, careful development procedures must be followed. The optimum exposure and processing are inseparable parameters. First, diffraction efficiency is peaked by aiming for $T_A = .4$ or a density of 0.8. The operating range $0.2 < T_A < 0.5$ will be linear and should contain all recorded data. An exposure of 30 to 40 ergs/cm^2 is required for Agfa 10E75 and 100 to 150 ergs/cm^2 for Agfa 8E75. The computation of required exposure time for a CW laser is straightforward. This is the so-called bias point.

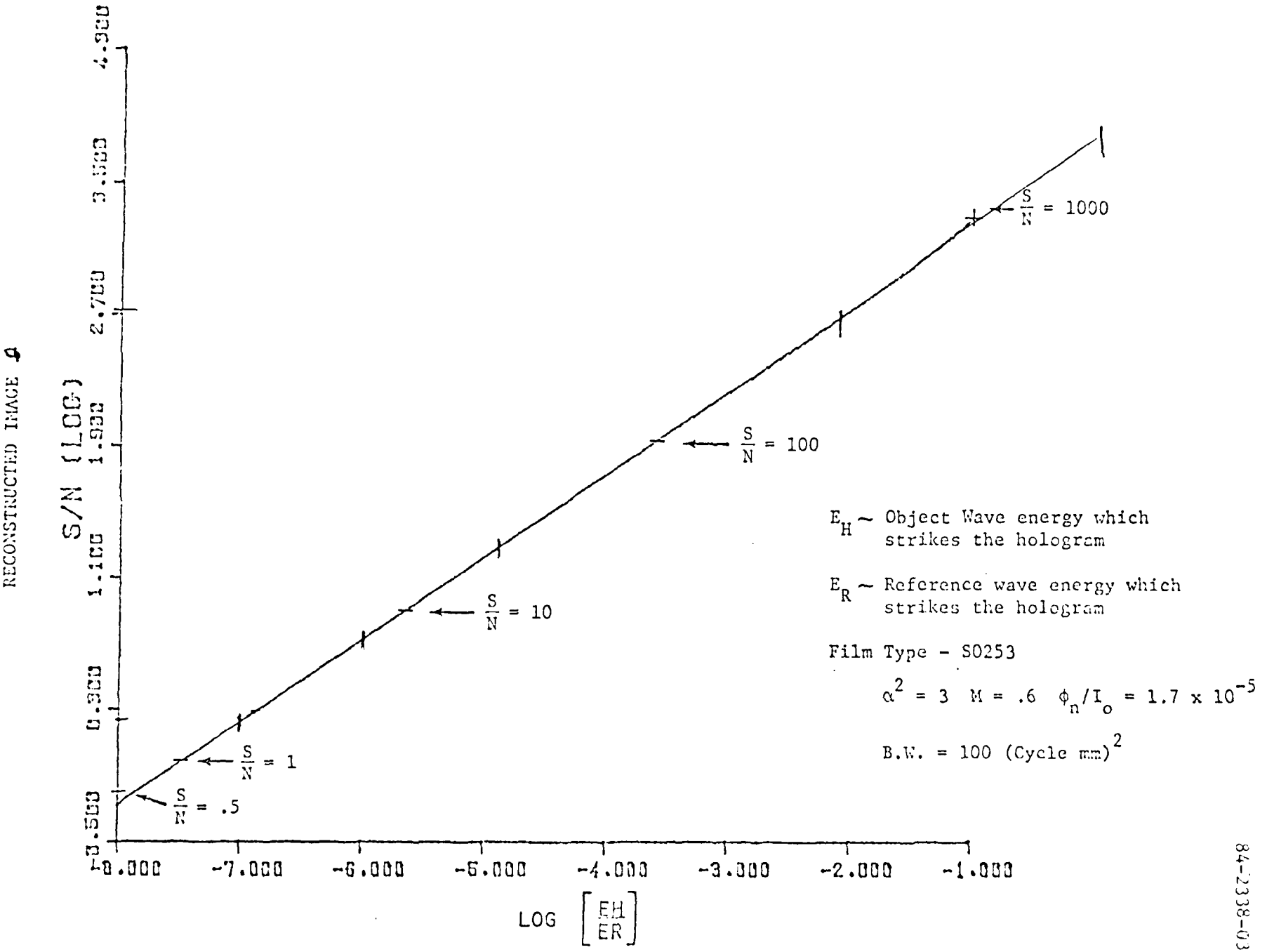

Figure 3. Signal to Noise Ratio. In reconstructed Image vs. Ratio

84-2338-03A-2

The most refined hologram processing methods commonly known include the following points which are uncommon in ordinary photography.

1. Used degassed, distilled water.
2. Discard developer after use.
3. Monitor photographic density during development and stop at the chosen density.
4. A final washing in distilled water.
5. Drying at room temperature.
6. Stress relieving before recording should be considered.
7. Latent image loss can be severe. Test should be run.

1.6 Summary for Hologram Optimization

Table II provides a summary for overall optimization of hologram quality.

Minimum Geometrical Requirements

Figure 4 illustrates the recording and reconstructing geometries for a hologram. The object and reference wave should impinge at equal and opposite angles with respect to the hologram normal (see Reference 1). If the reference wave and object wave (before striking the object) are both parallel, the basic spatial carrier frequency is

$$f_c = 2 \sin \psi_o / \lambda \quad .$$

This is the minimum requirement of the recording emulsion. The required bandwidth around the carrier can be computed if the effective hologram size is known, simply by calculating the largest and smallest angle

TABLE II

TECHNIQUES FOR IMPROVING HOLOGRAM QUALITY

WHERE APPLIED	SIGNAL TO NOISE RATIO	RESOLUTION
DESIGN	1. Use as few optical elements as possible. Low scatter elements 2. Baffel stray light 3. Spatial filter beams 4. Choose an emulsion with low noise, high MTF, high Gamma 5. Have reference wave at least 10 times object wave 6. Object reference angle is bisected by plate normal 7. Object/reference angle larger than subtended object angle	1. Hologram size must be large enough 2. Emulsion resolution high 3. Low object/reference beam angle 4. Use flat plates 5. Place object close to hologram 6. Use direct (not diffuse) light 7. High quality optics (flatness, parallelism, good lenses) 8. Image and magnify the object before recording 9. High coherence
DURING RECORDING	1. Keep everything clean in the optical train 2. Maintain uniform intensity wavefronts 3. Put as little as possible in the object field 4. Expose optimally	1. Keep everything stationary to $\lambda/10$ 2. Keep windows thin and go through them straight
DURING PROCESSING	Develop to transmissivity of .16-.20 Shorten development time Maintain cleanliness Final distilled water wash	Same as for high S/N
DURING PLAYBACK	1. Keep optical train free of dust 2. Uniform beams 3. Use a liquid gate 4. Illuminate only the part of hologram required 5. Spatial Filter	1. Orient hologram position precisely 2. Use real image corrected by projecting backwards through any optics originally used 3. Use correct wavelength 4. Duplicate original reference wave

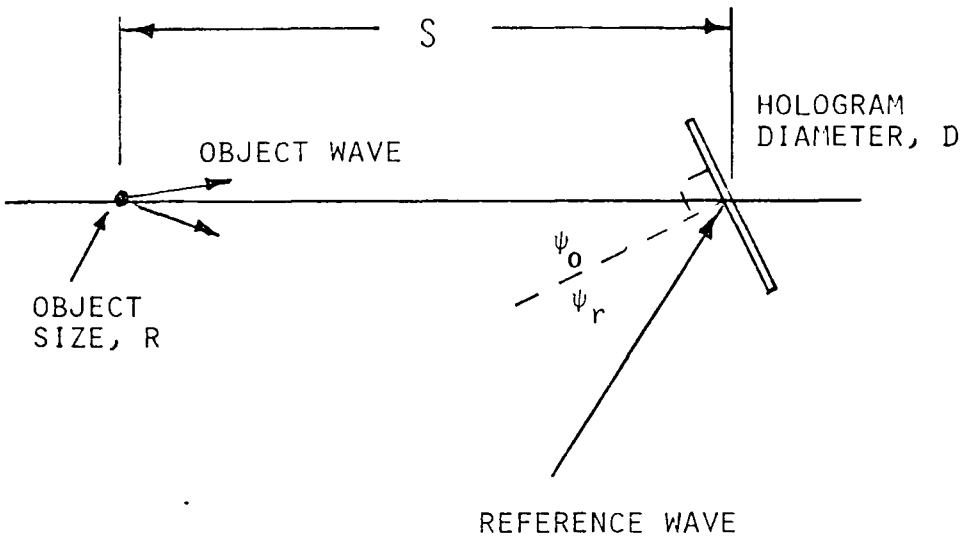

(A) FORMATION

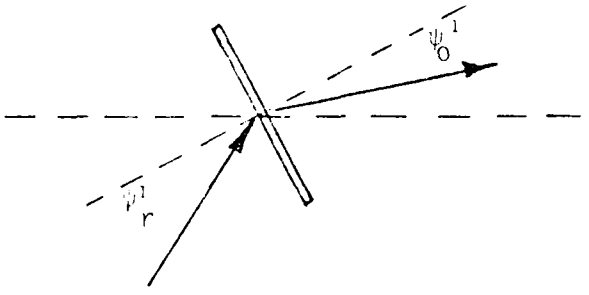

(B) RECONSTRUCTION

FIGURE 4. - HOLOGRAM GEOMETRY

between the object and reference wave. Then the two dimensional bandwidth which is used to compute total noise is the square of the one dimensional case. This one dimensional bandwidth is given approximately by

$$B_1 = \frac{4}{\lambda}\left[\sin\left(\psi_o + \tan^{-1}\frac{D}{2S}\right) - \sin\psi_o\right] \quad .$$

The required effective diameter for the hologram is proportional to the required resolution, R.

$$D_{req} = \frac{1.2\ S\lambda}{R\ \cos\psi_o} \quad .$$

Higher resolution requirement demands either a larger effective hologram diameter or a smaller object distance, S.

Parameters for this Experiment

Carrier Frequency The angle between the object and reference waves is 40 degrees. Hence,

$$f_c = \frac{2\ \sin 20}{.63 \times 10^{-3}\ \text{mm}} = 1085\ \text{lines/mm} \quad .$$

Bandwidth The object distance, S, is approximately 15 mm from a hologram of diameter, 10 mm.

$$B_1 = \frac{4}{.63 \times 10^{-3}\,mm} \left[\sin (20 + 16) - \sin 20\right] = 1523 \quad .$$

The two dimensional bandwidth is

$$B_1^2 = 2.32 \times 10^6 \quad .$$

Maximum Spatial Frequency

Assuming that the hologram diameter is the limiting factor

$$f_m = f_c + \frac{B_1}{2} = 1846 \text{ lines/mm} \quad .$$

Actually the image transfer system is more restrictive than this, meaning that 1846 lines/mm is more than will be required of the hologram. In reconstructing, any bandwidth passed above the recording lens transfer system adds only noise to the image.

Image Self-Interference Frequency

At the center of the hologram the angle subtended by the object is 1 tan 0.3 = 33 degrees. Since the angle between the object and reference wave is 40 degrees, the noise spectrum for self-interference lies below the basic carrier frequency and will not appear in the reconstructed image (assuming that the recording is linear).

Summary

The recording medium requires a resolution of 1846 lines/mm. Either Agfa 10E75 or 8E75 will accommodate this with a nearly peaked MTF. The basic carrier frequency will be 1085 lines/mm.

The resolution for the hologram will be limited by the image transfer system to approximately 4 microns. This could be reduced, if needed, by using a higher resolution image transfer.

Lens Configurations and Image Transfer in Holography

In an imaging holocamera the possibilities for positioning and magnifying the image before and after reconstruction are many and it is important to understand how these affect the ultimate appearance of the data. It is extremely important to know in advance the probable location of the image. This can save a vast amount of confusion and delay during the reconstruction. It also allows one to optimize the reconstructed data for whatever recording or viewing system is used. Three classes of imaging systems must be considered.

1. A collimator pair which images one-to-one in 3 dimensions. This was the configuration used in the present system.
2. A collimator pair which magnifies such that the magnification in the image field is uniform everywhere but the magnification is not the same in the depth dimension as it is in the planar dimension. The magnification is the ratio of the focal lengths of the two collimators used.
3. Use of the single lens to image and magnify before reconstruction.

In the following discussion each of these lens systems and its imaging properties is described in detail. For the first part of this discussion the hologram itself is not mentioned. The reader must only remember that the hologram itself only recreates what exists optically, so in any of these discussions the hologram position could be at any place in the entire diagram. Ideally, with or without the hologram, the image space stays the same. One can consider the image space as being produced by the alignment laser and the holocamera lenses when the hologram is not present, or being produced by the hologram when it is set up in a reconstruction system. From an optics point of view, when the optical wave from the hologram is examined one cannot discern whether it has come from the hologram or from the imaging system in the holocamera. The two ideally should be identical.

Figure 5 describes the imaging properties of a collimator pair which images 1 to 1 in 3 dimensions. This system allows the largest field of view and because the image space is identical to the object space it is the simplest system to analyze.

There are 3 separate cases that must be considered when the two matched lens collimator pair is used. Case 1, which is illustrated in Figure 5a and in Figure 5b, has a sample space defined by a volume that is two focal lengths long and one lens diameter wide. The hologram can be positioned anywhere on the right hand side of the second lens. In some cases where an image plane hologram is desirable the image of the sample volume exists on both sides of the hologram, as shown in Figure 5b. As previously mentioned it is sometimes convenient to position the hologram such that all of the sample space appears on only one side of

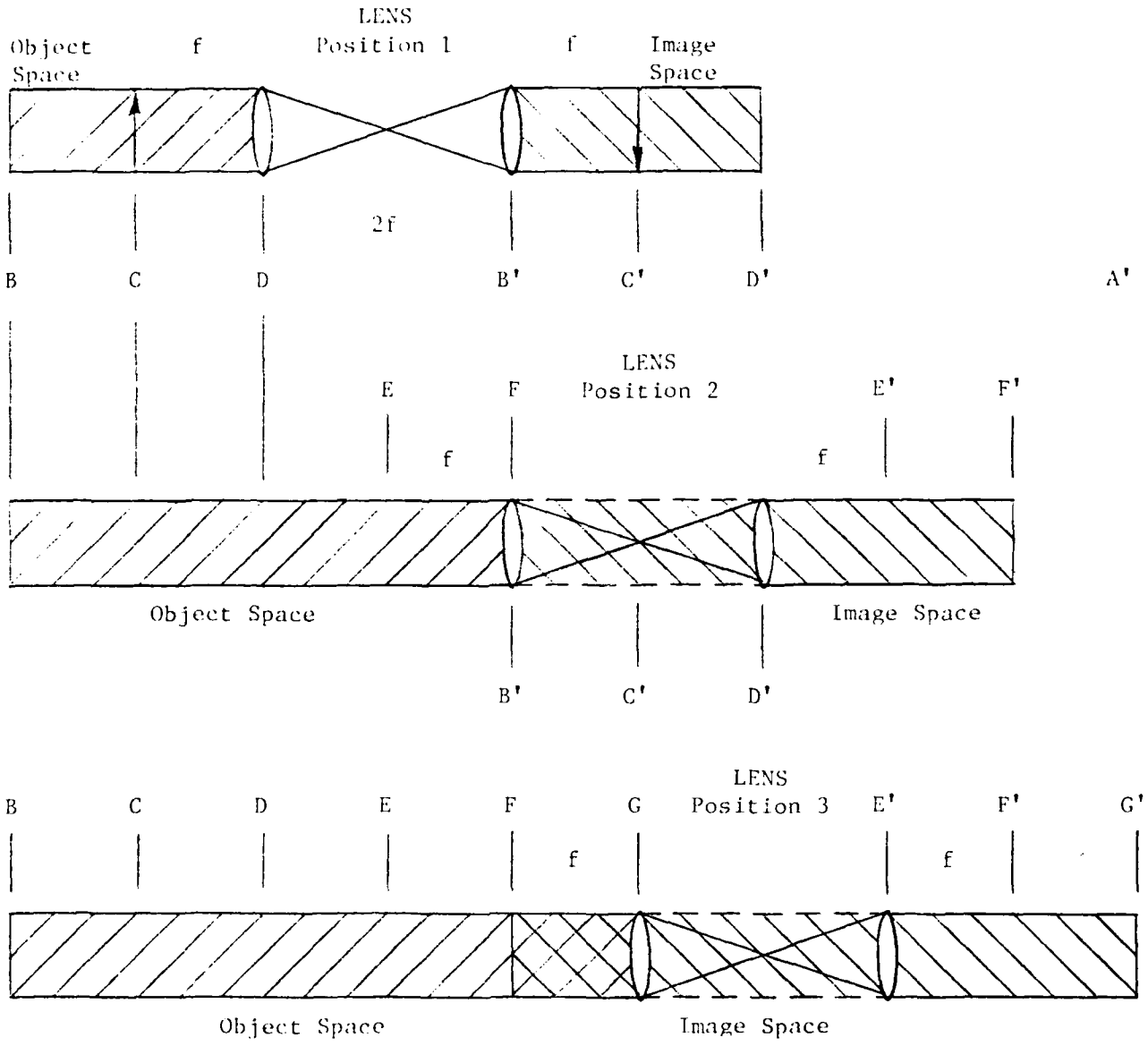

Object Space is represented by A, B, C, D, E, F, G. The corresponding image (congugate) Points are primed (A', B', etc.) respectively. Note that the relative positions of the object and image space are fixed regardless of the location of the lens pair! In lens position 3 note that the object and image spaces overlap.

FIGURE 5a. ONE-TO-ONE IMAGING IN THREE DIMENSIONS WITH A MATCHED COLLIMATOR PAIR

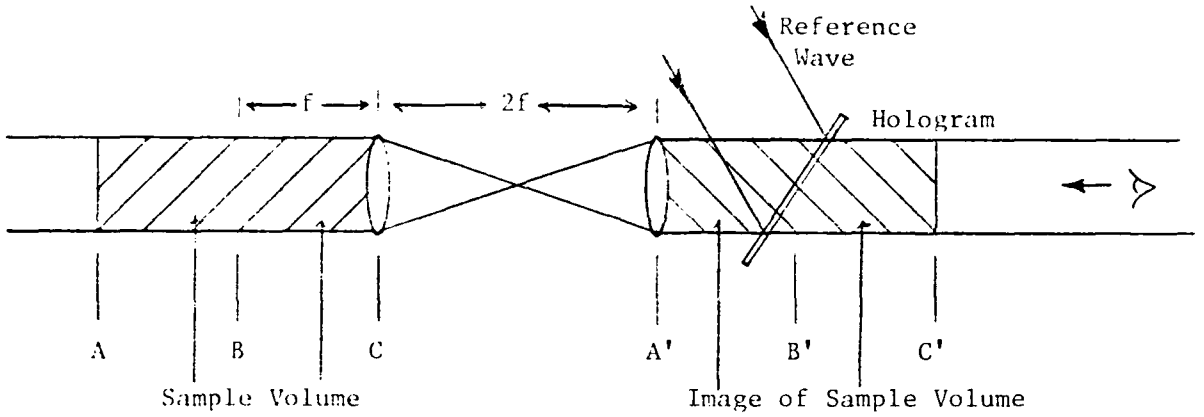

CASE 1: RECORDING WITH TWO COLLIMATORS

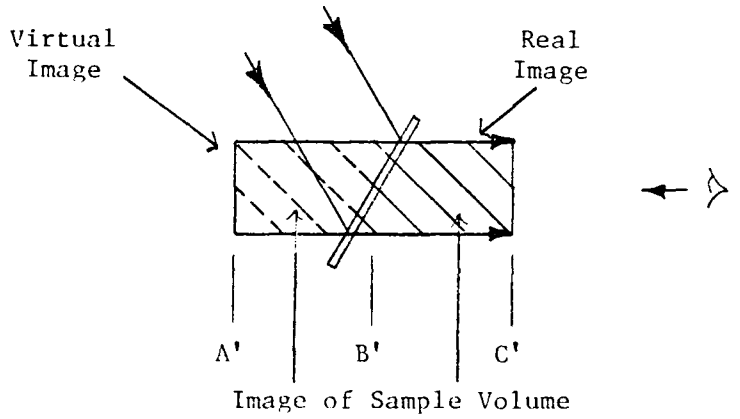

RECONSTRUCTING THE ORIGINAL WAVE

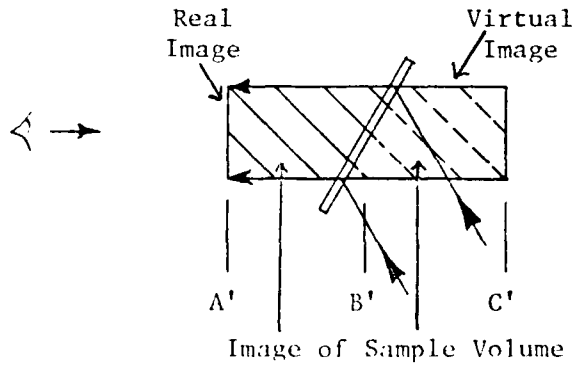

RECONSTRUCTING A CONJUGATE OF THE ORIGINAL WAVE

FIGURE 5b. HOLOGRAPHY WITH A ONE-TO-ONE IMAGING SYSTEM

the hologram. When the image exists on both sides of the hologram part of it is a real image and part of it is a virtual image. The real image can actually be presented directly to a frosted screen for viewing or directly to a lensless camera. The virtual part of the image must be reimaged into a real image before viewing on a frosted screen or recording.

The part of the image that is virtual can be made real in holography simply by reversing the direction of the reference wave and projecting backwards through the hologram as shown in the third figure of Figure 5b. In this case the reference wave comes from the right and the viewer sees the reconstructed image on the left hand side of the hologram. The part of the image that was virtual now becomes real. This process is often useful when presenting an image directly to the face of the vidicon without using other lenses where part of the field of interest happens to exist behind the hologram in a virtual space. This procedure allows one, by turning the hologram over, to convert this virtual space into a real space.

The two lens image method just described applies both lenses before the recording of the hologram. In an equivalent technique one can apply one of these lenses before a holographic recording and the other during holographic reconstruction. This is illustrated in Figure 5c. The recording is made with the hologram in a position just forward of where the second collimator would have been placed, for example, as shown in Figure 5c. The diverging wave is then recorded in the hologram. During reconstruction the reconstructed wave will be that diverging wave. The collimator which was used during recording can then

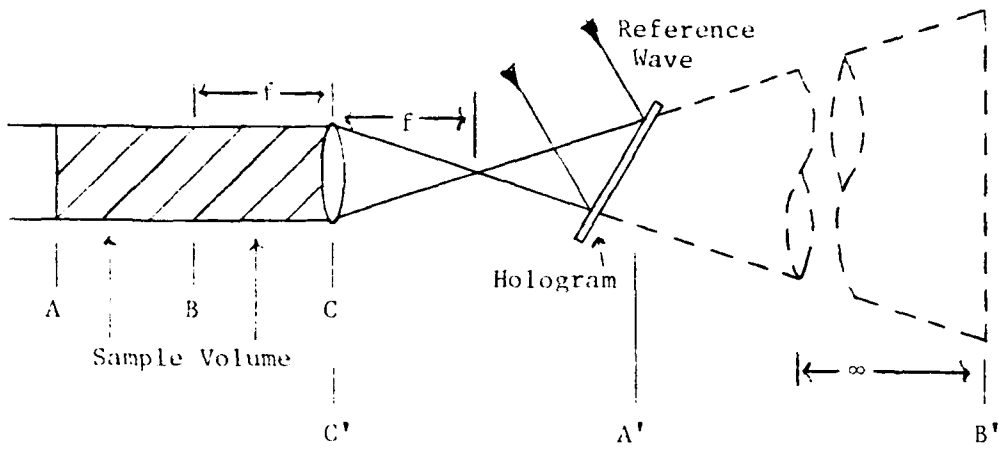

CASE 2: RECORDING WITH ONE COLLIMATOR

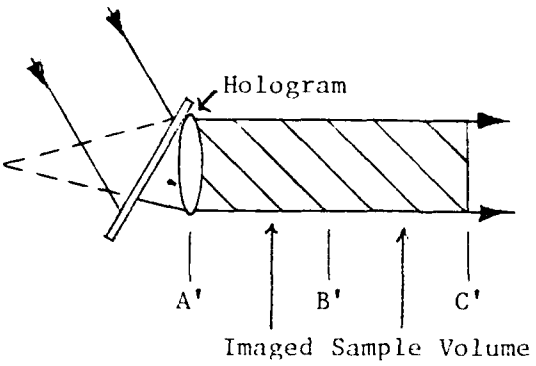

RECONSTRUCTING ONE TO ONE WITH THE SECOND COLLIMATOR BEING SUPPLIED DURING RECONSTRUCTION.

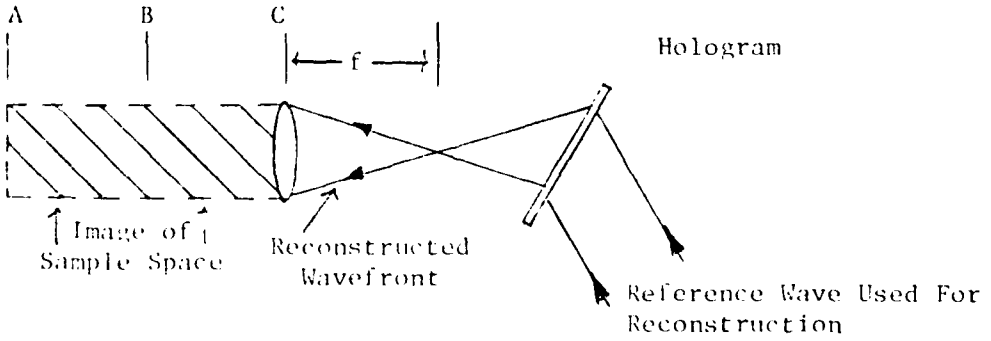

REMOVING LENS ABERRATIONS DURING RECONSTRUCTION

FIGURE 5c. USING ONE LENS DURING RECORDING AND THE SAME LENS DURING RECONSTRUCTION TO ACHIEVE ONE-TO-ONE IMAGING.

be used as an exact matched collimator to collect this diverging wave and recollimate it, producing a one to one image of the original sample volume. The points A', B', C' in this image correspond to the original A, B, and C, in the sample volume.

When it is desired to produce an image of ultimate quality, removing any defects that may exist in the collimator as an imaging element, the technique used in the bottom figure produces a so-called conjugate wave traveling antiparallel to the original wave to be projected backwards through the collimator used during recording. Aberrations that were impressed upon this wave during its original transmission by the lens are then removed before the image appears once again in the original sample space free of geometric aberrations.

Figure 6 illustrates the process of imaging with magnification. Two separate cases need to be considered, one in which the image space is a constant magnification of the object space and the other in which the magnification of the object space depends upon the location in that space. The top diagram illustrates the imaging for the former case. Here two collimators with different focal lengths are used taking a collimated wave from the object space and reproducing a collimated wave in the image space. The magnification is the ratio of the two focal lengths. This is the magnification for the x and y dimensions. Magnification in the z dimension can be seen from this diagram to be the square of the magnification of the x and y dimensions. For the lens shown, therefore, magnification in the x and y dimensions is 3 while magnification in the z dimension is a 9. For example, the distance BC is imaged B', C', nine times the original object dimension. This type

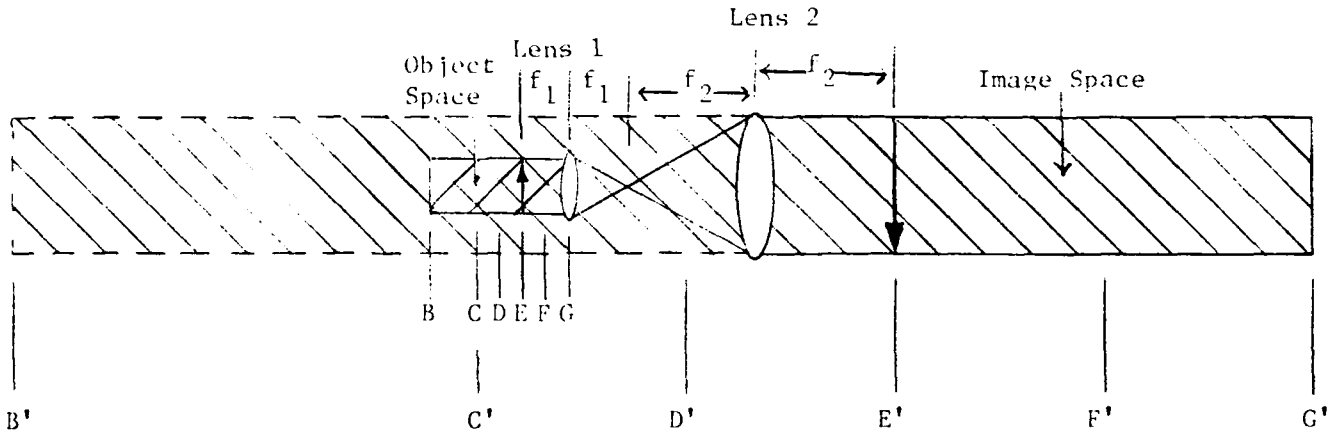

IMAGING WITH TWO LENSES TO PRODUCE CONSTANT MAGNIFICATION.

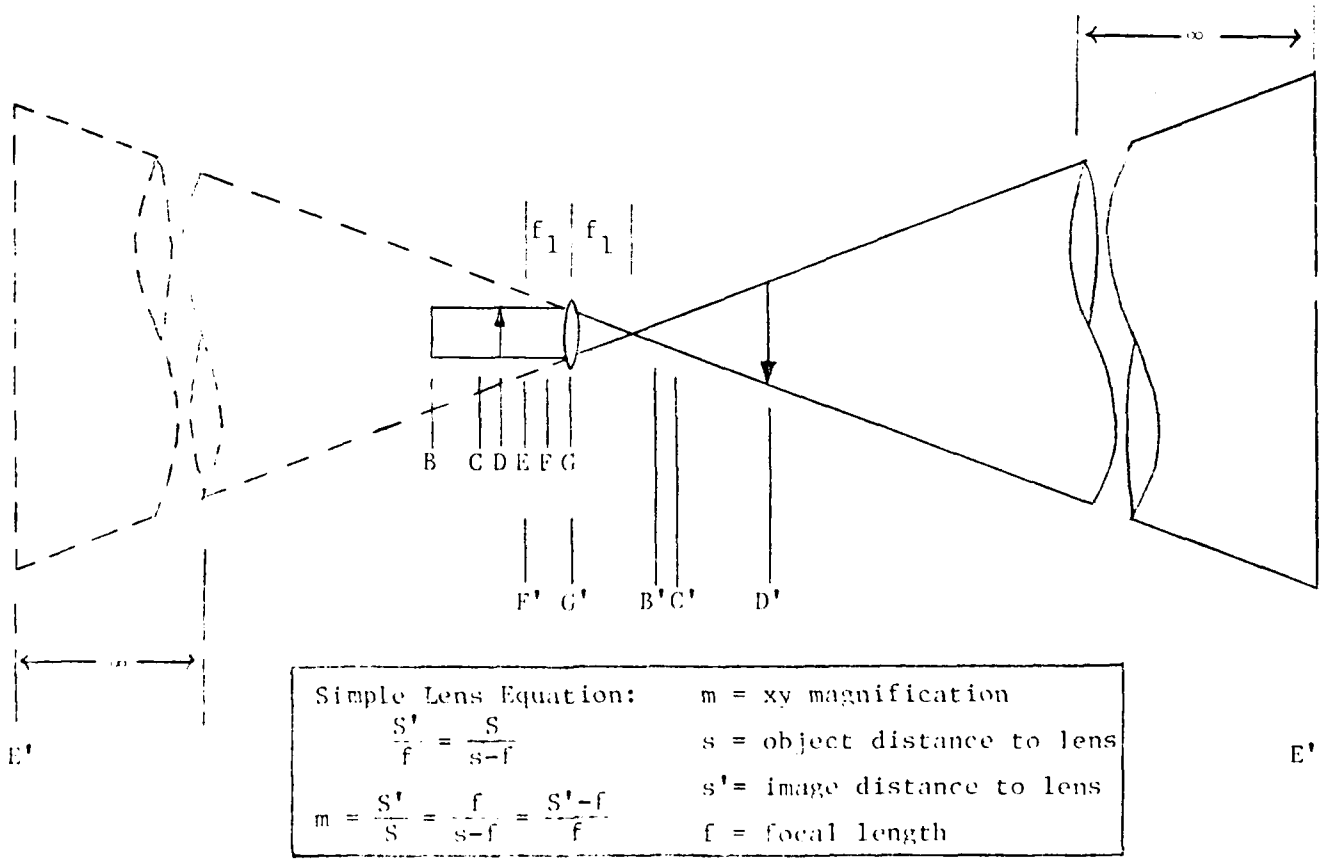

Simple Lens Equation: $\frac{S'}{f} = \frac{S}{s-f}$	m = xy magnification
	s = object distance to lens
	s'= image distance to lens
$m = \frac{S'}{S} = \frac{f}{s-f} = \frac{S'-f}{f}$	f = focal length

IMAGING WITH A SINGLE LENS PRODUCING MAGNIFICATION WHICH VARIES WITH AXIAL POSITION.

FIGURE 6. IMAGING WITH MAGNIFICATION

of lens configuration is extremely useful because the image space is magnified by a constant value independent of the position in the original object space. The volume lying from one focal length in front of the short lens up to the surface of the small lens is imaged to the right hand side of the large lens in a space which is convenient for producing holograms. As with the previous lens the hologram can be positioned at any place in the image space. Precisely the same method for handling the reconstructed image for the matched collimator pair can be used here. If any part of the image is a virtual image in the reconstruction, it can be converted to a real image simply by reversing the direction of the reconstruction reference wave, a practice which is achieved normally by turning the hologram over. The stretching out of the image space in this reconstruction does make the analysis of the reconstructed image require more space if the object itself has considerable z dimension. When such is the case, it is often better to reconstruct the wave back through the lens pair to create an image space identical to the original object space.

When an object field is magnified with a single lens, the amount of magnification depends upon the position of the object. The closer the object is to the focal point of the lens the greater the magnification. When a very thin object field is used this creates little problem since the amount of magnification is easy to determine simply by knowing where the object or image field is. The equations are provided in Figure 6. The magnification is simply the ratio of the image to object distance or when either the image or the object distance alone is known then one of the other two relationships for magnification

can be used. For example, if only the image distance is known, as might be the case in observing a reconstructed image, the magnification is provided by the difference between the image distance and the focal length divided by the focal length.

When a larger sample volume is desired with magnification, it is sometimes convenient to produce a constant magnification image space. This can be done either during recording, as illustrated in the top figure of Figure 6, or during reconstruction, as illustrated in Figure 7.

By studying Figures 5 through 7, it is easy to see how, by using different lens configurations, the image space of the hologram can be located almost anywhere. Without some predetermination of this image space location it is likely to occur in in an inconvenient space and require reimaging. Locating the image space can be done by using the relationships shown in these figures or as described previously by inserting the calibration object in the object space and observing the location of its image relative to the hologram.

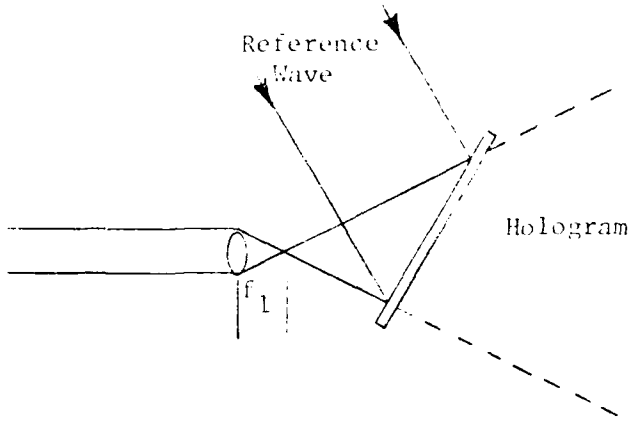

CASE 3: RECORDING WITH ONE MAGNIFIER

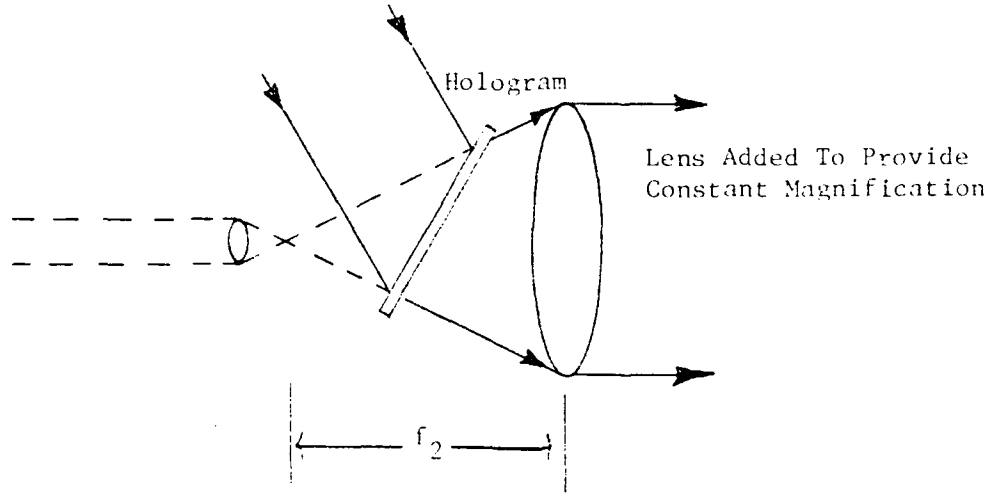

NORMAL RECONSTRUCTION

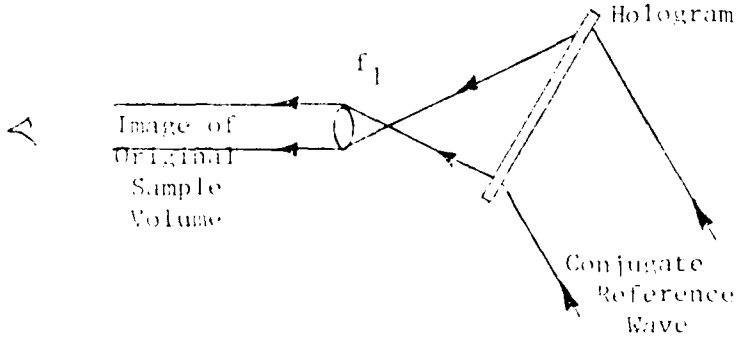

RECONSTRUCTION BACK THROUGH THE ORIGINAL PATH

FIGURE 7. HOLOGRAPHY WITH PREMAGNIFICATION

REFERENCES

1. J. D. Trolinger, "Analysis of Holographic Diagnostics Systems," Optical Engineering, 19, 722, (1980)

2. "Holographic Recording Materials", Topics in Applied Physics, Vol. 20 (1977).